

Figure 2

The ET-1/ET_A receptor augments NGF expression via Giβγ, PKC, EGFR, ERK, p38MAPK, and AP-1 and C/EBPδ elements. (A) Preincubation of cardiomyocytes with either PTX or H89. NGF mRNA expression was determined 2 hours after ET-1 stimulation. (B) Cardiomyocytes were pretreated with LacZ or BARK-ct to inhibit the function of Giβγ, and stimulated with ET-1. BARK-ct attenuated ET-1-induced NGF expression, but not BNP. (C and D) Stimulation with PMA (a PKC activator) for 2 hours augmented NGF expression. In contrast, pretreatment with chelerythrine (che; a PKC inhibitor) for 30 minutes or PMA for 24 hours inhibited ET-1-induced NGF expression. (E and F) Pretreatment with PD98059 (PD; an MAPK inhibitor), AG1478 (AG; an EGFR inhibitor), SB203580 (SB; a p38MAPK inhibitor), or PP2 (an Src family inhibitor), but not with wortmannin (WM; a PI3K inhibitor) or KN62 (a calmodulin kinase II/IV inhibitor) attenuated ET-1-induced NGF mRNA expression. BNP was affected only with PD98059 pretreatment. (G) The results of the densitometry of four separate experiments are shown. *P < 0.001 vs. control; **P < 0.01 vs. ET-1 alone. NS, not significant vs. ET-1 alone. (H and I) Cardiomyocytes were pretreated with DN-ERK or DN-p38MAPK. (J and K) Identification of ET-1-responsive elements in the NGF promoter using luciferase assay. Black bars, control; white bars, ET-1 stimulation (n = 4). (L) Specific negative regulatory plasmid of the EGFR (533delEGFR) or the Src family (Csk) inhibited NGF transcription (n = 4). *P < 0.001, **P < 0.01, *P < 0.05 vs. relative control. NS, not significant.

inhibitors, indicating that this pathway is clearly distinct from pathways that mediate hypertrophy. Transfection of DN-ERK or DN-p38 strongly attenuated NGF induction, showing that extracellular signal-regulated kinase (ERK) and p38MAPK are critical in this augmentation (Figure 2, H and I).

The NGF promoter contains both activator protein-1 (AP-1) and CCAAT/enhancer-binding protein δ (C/EBPδ) elements (18). ET-1 augmented luciferase activity from the full-length NGF promoter (-615/+50) 4.0-fold, but deletion of the AP-1 element markedly decreased this augmentation (Figure 2J). The truncation plasmids revealed that the C/EBPδ element was also involved in this induction, but that the AP-1 element was more critical. Other hypertrophic factors did not induce NGF transcription (Figure 2K). Cotransfection of luciferase under the influence of the NGF promoter with a mock plasmid or with the Csk or the 533delEGFR plasmid revealed that Src- and EGFR-mediated signaling was involved in NGF induction (Figure 2L). These results indicate that

Giβγ, PKC, the Src family, EGFR, ERK, p38MAPK, C/EBPδ, and the AP-1 site are critically involved in this signal transduction pathway.

ET-1 augments NGF-induced differentiation of PC12 cells through NGF secretion from cardiomyocytes. PC12 cells, a rat pheochromocytoma cell line that responds with neurite extension to NGF, was used to assay conditioned medium. To determine whether ET-1-induced NGF production in cardiomyocytes is a biologically relevant phenomenon, we stimulated PC12 cells with conditioned medium for 3 days and examined cell morphology (Figure 3A). Medium conditioned with ET-1-stimulated cardiomyocytes significantly induced neurite outgrowth compared with medium conditioned with unstimulated cardiomyocytes (Figure 3B). Pretreatment of PC12 cells with anti-NGF blocking antibody strongly suppressed cell differentiation (Figure 3C). To mimic sympathetic innervation in the heart, we cocultured PC12 cells with cardiomyocytes and stimulated them with ET-1. PC12 cells showed differentiation that was inhibited by pretreatment with anti-NGF blocking antibody

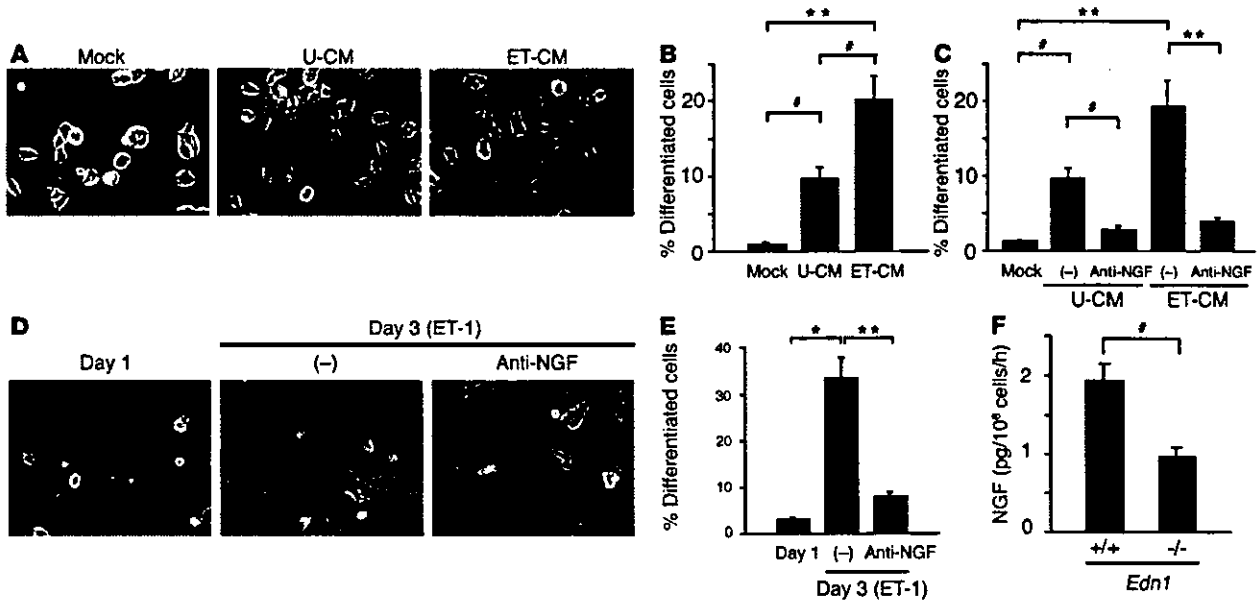


Figure 3

ET-1 causes NGF-mediated differentiation of PC12 cells. (A) PC12 cell morphology was observed after incubation for 3 days in mock medium or medium conditioned with unstimulated cardiomyocytes (U-CM) or ET-1-stimulated cardiomyocytes (ET-CM). Medium conditioned with ET-1-stimulated cardiomyocytes strongly induced neurite extension in PC12 cells compared with medium conditioned with unstimulated cardiomyocytes. (B) Percentage of differentiated cells in A ($n = 4$). (C) PC12 cells were pretreated with anti-NGF blocking antibody for 30 minutes, then incubated with the conditioned medium ($n = 4$). (D) PC12 cells transfected with LacZ were cocultured with cardiomyocytes, then stimulated with ET-1 or ET-1 plus anti-NGF blocking antibody for 3 days. PC12 cells were identified using X-gal staining. (E) Percentage of differentiated cells in D ($n = 4$). (F) NGF protein levels in medium conditioned with *Edn1*^{+/+} or *Edn1*^{-/-} cardiomyocytes were measured by ELISA ($n = 4$). * $P < 0.0001$; ** $P < 0.001$; # $P < 0.01$. Scale bar: 100 μ m.

(Figure 3, D and E), indicating that the NGF secreted by cardiomyocytes is capable of stimulating neuriteogenesis in PC12 cells.

To investigate whether endogenous ET-1 secreted by cardiomyocytes is critical for NGF production, we measured the NGF protein level in medium conditioned with *Edn1*^{-/-} or *Edn1*^{+/+} cardiomyocytes and found it to be reduced by half in medium conditioned with *Edn1*^{-/-} cardiomyocytes (Figure 3F).

Disruption of ET-1, but not angiotensinogen, reduces NGF expression, sympathetic nerve density, and norepinephrine concentration in the heart. To investigate whether ET-1-specific induction of NGF in cardiomyocytes participated in cardiac sympathetic nerve development, we analyzed *Edn1*^{-/-} mouse hearts at embryonic day (E) 18.5. *Atg*^{-/-} mice were used as a control. The levels of NGF mRNA in *Edn1*^{-/-} mouse hearts were downregulated to 32% of those in *Edn1*^{+/+} hearts (Figure 4A), while those in *Atg*^{-/-} mice showed no change (97% of those in *Atg*^{+/+} mice). The mRNA levels of neurotrophin-3, another neurotrophic factor known to induce sympathetic innervation (28), were unaffected in *Edn1*^{-/-} and *Atg*^{-/-} mice (Figure 4B).

To determine the cardiac sympathetic nerve density in these mice, immunostaining was conducted using antibodies to TH, a marker for sympathetic nerves, GAP43, a marker for nerve sprouting, and PGP9.5, a general marker for peripheral neurons. Immunostaining for TH, GAP43, and PGP9.5 was performed on serial sections and labeled the same structures in several areas of the heart (data not shown), as described previously (7, 8). At E18.5, most sympathetic nerve endings were restricted to the epicardium in both *Edn1*^{-/-} and *Atg*^{-/-} mice. Surprisingly, GAP43, PGP9.5, and TH immunoreactivities were markedly decreased only in *Edn1*^{-/-} mice (Figure 4, C–F).

The concentration of total cardiac norepinephrine was significantly lower in *Edn1*^{-/-} mice than in *Edn1*^{+/+} littermates but was unaffected in *Atg*^{-/-} mice (Figure 4G). These results indicated that NGF expression and cardiac sympathetic innervation are specifically reduced in *Edn1*^{-/-} hearts.

ET-1-deficient mice display a loss of SG neurons by apoptosis during periods of NGF dependence. The cardiac sympathetic nerve extends from the sympathetic neurons in SG, which are derived from neural crest cells. Neural crest cells migrate and form sympathetic ganglia by E11.5, then proliferate and differentiate into mature neurons. To examine whether ET-1 affects the early stage of sympathetic trunk formation in SG, we immunostained whole-mount *Edn1*^{-/-} embryos with anti-TH antibody at E12.5 (Figure 5A). TH⁺ neurons formed normal ganglia and sympathetic trunks bilaterally to the vertebra. Next, we examined the size and cellularity of SG by cresyl violet staining and immunostaining for TH (Figure 5, B, C, and F). At E12.5 and E15.5, neuronal cell counts and area were unaffected in *Edn1*^{-/-} SG compared with WT. Moreover, TH immunoreactivities were not changed in *Edn1*^{-/-} SG, indicating that migration and differentiation of neural crest cells in SG were not disrupted in the early stages. At E18.5, however, *Edn1*^{-/-} SG were markedly smaller than those found in WT embryos, contained fewer neurons (55% of WT), and had a mean neuronal area that was 73% smaller than that of WT embryos. Thus, *Edn1*^{-/-} SG exhibited a dramatic loss of sympathetic neurons between E15.5 and E18.5. To examine the cause of the loss of SG neurons in *Edn1*^{-/-} embryos, sections were processed with Ki-67 immunostaining to assess the level of proliferation (Figure 5, D and G). *Edn1*^{-/-} SG displayed nearly identical levels of proliferation compared with WT at

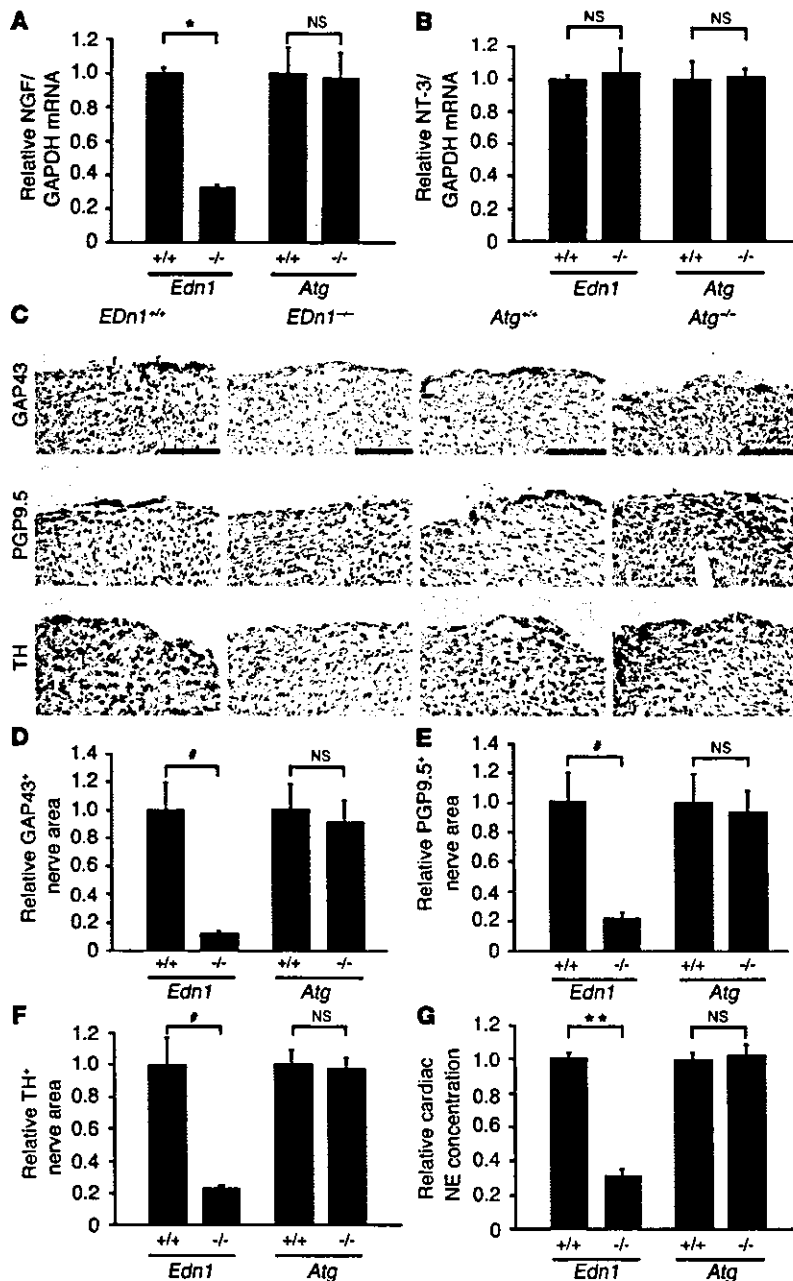


Figure 4 Disruption of ET-1, but not of angiotensinogen, reduces NGF expression, sympathetic nerve density, and norepinephrine concentration in murine hearts. (A) NGF expression in *Edn1*^{+/+}, *Edn1*^{-/-}, *Atg*^{+/+}, and *Atg*^{-/-} hearts at E18.5 was determined by quantitative RT-PCR (n = 10). (B) Neurotrophin-3 (NT-3) expression in the heart was measured by quantitative RT-PCR. The same reverse transcription products used in A were analyzed. (n = 10.) (C) Immunostaining for GAP43, PGP9.5, and TH in the heart. Nerves were restricted to the epicardium in both genotypes, and levels of GAP43, PGP9.5, and TH were lower in *Edn1*^{-/-} mice, but not in *Atg*^{-/-} mice, compared with WT littermates. (D–F) The immunopositive nerve areas for GAP43, PGP9.5, and TH were determined using NIH Image (n = 8). (G) Cardiac norepinephrine (NE) concentrations were measured by HPLC (n = 10). *P < 0.0001; **P < 0.05; #P < 0.01. NS, not significant. Scale bar: 100 μm.

detected from E12.5 and increased sequentially, but levels were similar in *Edn1*^{-/-} and *Edn1*^{+/+} hearts at the early stages. Sympathetic nerve endings were not detected at E12.5 (data not shown) and appeared from E15.5, but no difference was observed at this stage. These findings suggested that sympathetic nerve fibers initially reached the heart and that disruption of subsequent innervation was coincident with NGF downregulation in *Edn1*^{-/-} hearts between E15.5 and E18.5.

Cardiac-specific overexpression of NGF overcomes the defects of the cardiac sympathetic nervous system in Edn1^{-/-} mice. It is possible that the low sympathetic nerve density in the heart and excess apoptotic in SG neurons in *Edn1*^{-/-} mice are a direct effect of ET-1 deficiency. To address this question, we initiated a genetic rescue of cardiac NGF expression in *Edn1*^{-/-} mice to investigate whether the defects were caused by reduced NGF expression. Transgenic mice overexpressing rat NGF under the control of α-myosin heavy chain promoter were bred onto the *Edn1*^{-/-} background to restore NGF activity specifically to the hearts of *Edn1*^{-/-} embryos. *Edn1*^{-/-}/MHC-NGF mice died postnatally and had craniofacial defects similar to those observed in *Edn1*^{-/-} mice. Quantitative RT-PCR revealed that strong NGF expression, 14.5-fold that of the control mice, was detected

in *Edn1*^{-/-}/MHC-NGF hearts at E18.5 (Figure 6A). Immunostaining for TH (Figure 6, B and C), GAP43, and PGP9.5 (data not shown) showed that *Edn1*^{-/-}/MHC-NGF mice had hyperinnervation compared with *Edn1*^{-/-} littermates. The norepinephrine concentration was markedly increased in *Edn1*^{-/-}/MHC-NGF hearts (Figure 6D). These results show that cardiac-specific NGF overexpression restores sympathetic nerve density in *Edn1*^{-/-} hearts. Next, *Edn1*^{-/-}/MHC-NGF SG were examined by cresyl violet staining, immunostaining for TH and Ki-67, and TUNEL staining at E18.5 (Figure 6, E–G). Loss of sympathetic neurons and reduced neuronal area were completely overcome, and the level of TUNEL⁺ cells also decreased. These results sup-

ported that the requirement of NGF for the survival of sympathetic neurons begins at E16.5, we used TUNEL staining to address whether excess apoptosis accounts for the loss of neurons. At E12.5 and E15.5, excess apoptosis was not detected, but at E18.5, *Edn1*^{-/-} SG displayed a fourfold increase in the number of TUNEL⁺ cells compared with those of WT littermates (Figure 5, E and H). These results indicated that loss of sympathetic SG neurons in *Edn1*^{-/-} mice results from excess neuronal apoptosis in late gestation but not from a failure in neuronal migration, differentiation, or proliferation.

Next, we analyzed the time course of cardiac innervation and NGF levels in *Edn1*^{-/-} and *Edn1*^{+/+} hearts (Figure 5, I–K). NGF mRNA was

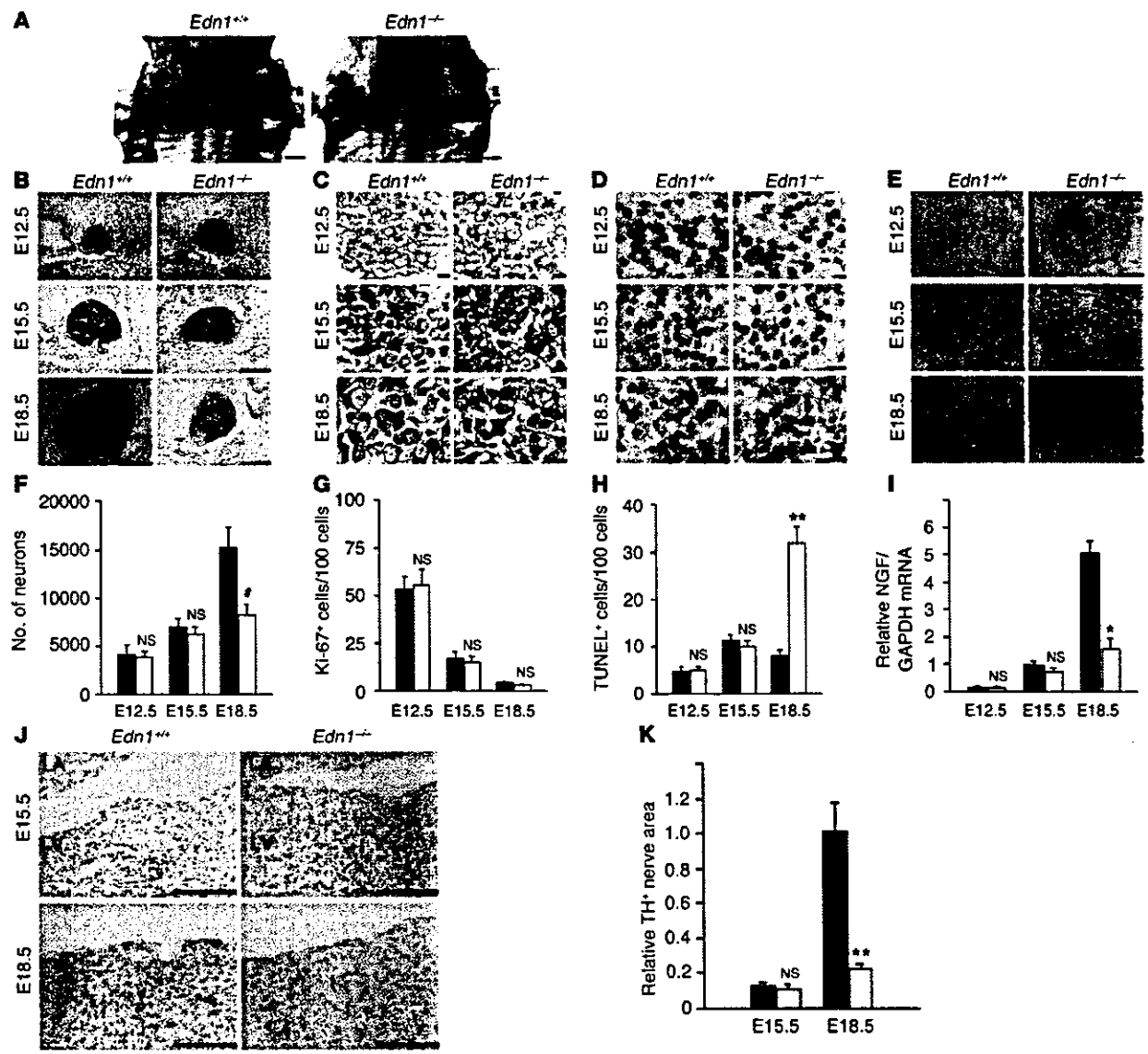


Figure 5 *Edn1*^{-/-} embryos display a loss of SG neurons due to excess apoptosis. (A) *Edn1*^{+/+} and *Edn1*^{-/-} whole-mount embryos at E12.5 were immunostained with anti-TH antibody. SCG, superior cervical ganglion; fl, forelimb. Similar results were obtained from four separate experiments. (B–E) TH immunostaining, cresyl violet staining (CV), Ki-67 immunostaining, and TUNEL staining of *Edn1*^{+/+} and *Edn1*^{-/-} SG at E12.5, E15.5, and E18.5 at the same level of section. Note that at E18.5, *Edn1*^{-/-} SG were considerably smaller than *Edn1*^{+/+} SG and increased apoptosis was detected. (F–H) Time course of the number of neurons, Ki-67⁺ cells per 100 neurons, and TUNEL⁺ cells per 1,000 neurons in SG was shown (*n* = 5). (I) Time course of NGF expression in *Edn1*^{+/+} and *Edn1*^{-/-} hearts was determined by quantitative RT-PCR (*n* = 3). (J and K) Immunostaining for TH in the heart of *Edn1*^{+/+} and *Edn1*^{-/-} embryos at E15.5 and E18.5. TH-immunopositive nerve fibers were slightly detected from E15.5. LA, left atrium; LV, left ventricle. The immunopositive nerve areas for TH were determined using NIH Image. (*n* = 4.) **P* < 0.001; ***P* < 0.01; **P* < 0.05. NS, not significant vs. relative control. Scale bar: 500 μm (A), 100 μm (B and J), 10 μm (C and D), 50 μm (E). Black bars, *Edn1*^{+/+}; white bars, *Edn1*^{-/-}.

port the hypothesis that the ET-1-NGF pathway plays a critical role in development of the cardiac sympathetic nervous system.

Discussion

Cardiac performance is tightly controlled by the autonomic nervous system. NGF is the best-characterized and most well-known member of the neurotrophin family, which contributes to the development and

maintenance of sympathetic innervation. The level of NGF synthesized in the target organ determines its innervation density (2). However, the molecular mechanisms that regulate NGF expression and sympathetic innervation remain poorly understood. In this study, we found that (a) ET-1, but not angiotensin II, phenylephrine, LIF, or IGF-1, induces NGF augmentation in cardiomyocytes; (b) ET-1-induced NGF augmentation is mediated by the ET_A receptor, Giβγ, PKC, the Src family,

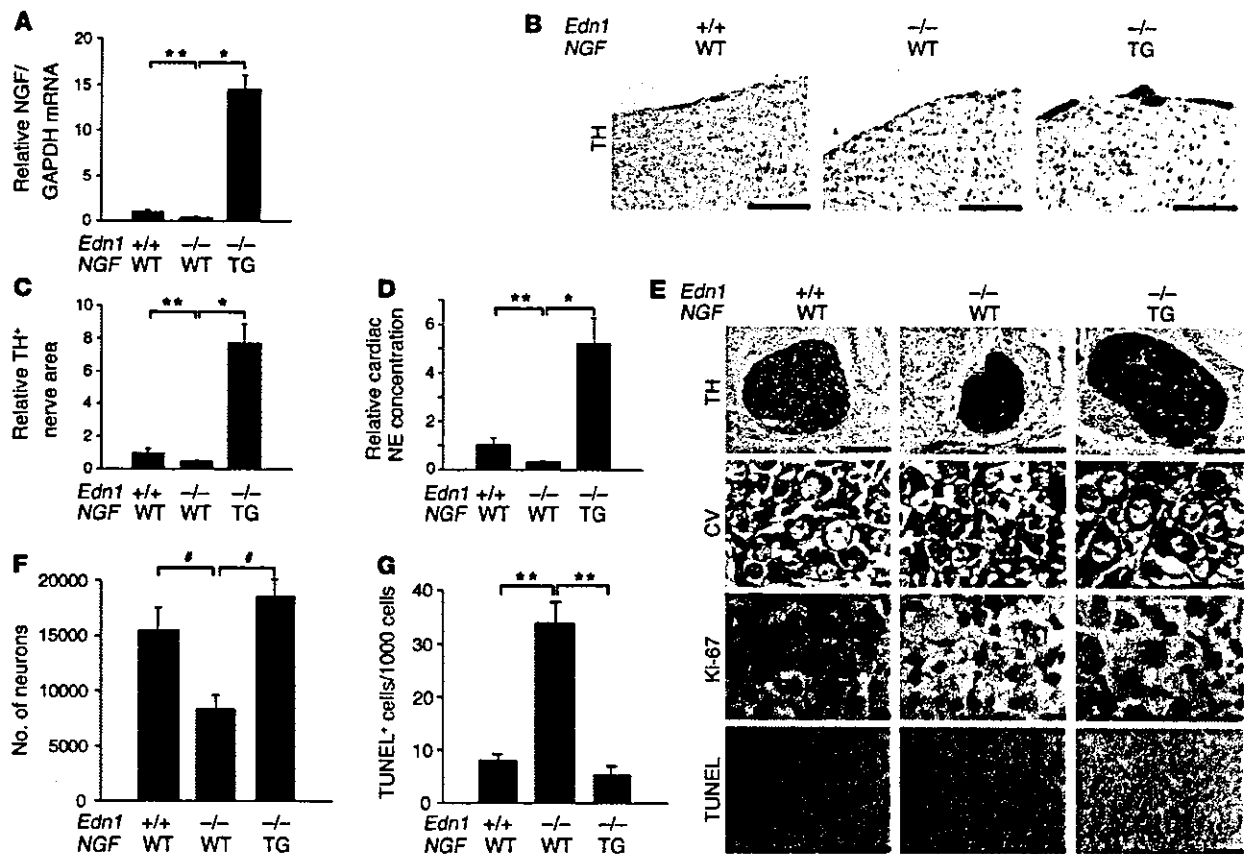


Figure 6 Cardiac-specific overexpression of NGF overcomes the defects of the cardiac sympathetic nervous system in *Edn1*^{-/-} mice. (A) NGF expression in *Edn1*^{+/+}, *Edn1*^{-/-}, and *Edn1*^{-/-}/MHC-NGF hearts is shown (*n* = 6). The reduced NGF expression in the *Edn1*^{-/-} heart was completely overcome by cardiac-specific overexpression of NGF. (B) Immunostaining for TH in the hearts of *Edn1*^{+/+}, *Edn1*^{-/-}, and *Edn1*^{-/-}/MHC-NGF mice. Scale bar: 100 μm. (C) The immunopositive nerve areas for TH were quantitated (*n* = 6). (D) The cardiac norepinephrine (NE) concentration was increased in *Edn1*^{-/-}/MHC-NGF mice compared with *Edn1*^{-/-} mice (*n* = 6). (E) TH immunostaining, cresyl violet staining (CV), Ki-67 immunostaining, and TUNEL staining of *Edn1*^{+/+}, *Edn1*^{-/-}, and *Edn1*^{-/-}/MHC-NGF SG at E18.5 at the same level of section. Note that the reduction of the size of SG and the increase in TUNEL⁺ cells in *Edn1*^{-/-} mice were completely reversed in *Edn1*^{-/-}/MHC-NGF mice. (F and G) The number of neurons and the number of TUNEL⁺ cells per 1,000 neurons in each SG are shown (*n* = 3–6). **P* < 0.0001; ***P* < 0.01; **P* < 0.05. TG, transgenic. Scale bar: 100 μm (TH), 50 μm (TUNEL), 10 μm (CV and Ki-67).

EGFR, ERK, and p38MAPK, but not by PKA, PI3K, or calmodulin kinase II or IV; (c) AP-1 and C/EBPδ elements are essential *cis*-elements for ET-1-induced NGF transcription, with AP-1 being the more critical of the two; (d) ET-1-induced NGF augmentation in cardiomyocytes stimulates the differentiation of PC12 cells; and (e) the analysis of *Edn1*^{-/-} and *Edn1*^{-/-}/MHC-NGF mice demonstrated that ET-1 is required for induction of NGF expression and for promotion of sympathetic innervation and survival of SG neurons. These results show that ET-1-specific regulation of NGF in cardiomyocytes plays a critical role in the development of the cardiac sympathetic nervous system.

Of the cardiac hypertrophic factors investigated in this study, only ET-1 augmented NGF expression, and the ET-1-NGF pathway was mediated by the ET_A receptor and Giβ. The ET_A receptor is known to activate Gs, Gq, and Gi proteins, while phenylephrine and angiotensin II activate Gq and Gs proteins (29). The characteristic coupling of the ET_A receptor to G protein subunits might explain the specificity of ET-1-induced NGF augmentation. In contrast to the present study, a previous study reported that the cAMP-PKA

pathway was involved in β-adrenoreceptor-mediated NGF augmentation in astrocytoma cells (30). The finding that ET-1 does not induce NGF augmentation in cardiac fibroblasts suggests that the NGF induction pathway is mediated in a cell type-specific manner.

In this study, we found that the differentiation of PC12 cells was enhanced when the cultures contained medium conditioned with ET-1-stimulated cardiomyocytes or were cocultured with cardiomyocytes treated with ET-1. Our results point to a critical role for ET-1-induced NGF production in the promotion of neurite extension. This is based on our finding that ET-1-induced neurite extension is completely blocked by anti-NGF antibody, and that ET-1 alone did not augment PC12 cell differentiation (data not shown). The blocking, by anti-NGF blocking antibody, of neurite extension induced by medium conditioned with unstimulated cardiomyocytes shows that cardiomyocytes secrete a basal amount of NGF.

Experimental sympathectomy does not alter the onset or extent of NGF mRNA accumulation in target organs, which indicates that regulation of NGF synthesis during development is independent of inner-



vation or norepinephrine secreted from sympathetic nerves (31). Upstream molecules that regulate NGF expression *in vivo* remain undetermined. The present study demonstrated that NGF was downregulated and sympathetic innervation in the heart was reduced in *Edn1*^{-/-} mice, but not in *Atg*^{-/-} mice. Moreover, in *Edn1*^{-/-} mice, SG that contribute to the sympathetic innervation of the heart revealed neuronal loss due to excess apoptosis at the late embryonic stage, but not due to failure in neuronal migration, differentiation, or proliferation. These findings are consistent with previous reports that increased pyknosis is detected from E16.5 in NGF-targeted mice and that NGF transported from target organs acts on survival of innervating neurons, but not on proliferation or differentiation of sympathetic neurons (24). Developing axons are guided to their targets and maintained by extracellular molecules. Neurotrophin-3 is also a critical factor for the survival and differentiation of sympathetic neurons (2, 5, 28). However, neurotrophin-3 was not downregulated in *Edn1*^{-/-} heart, and the sympathetic neuronal defects revealed in *Edn1*^{-/-} mice were restored by overexpression of NGF in the heart. Taken together, these findings suggest that ET-1 is a key regulator of NGF induction in the heart and plays a specific and critical role in construction of the cardiac sympathetic nervous system via the regulation of NGF production. To our knowledge, this is the first report to identify a molecule that regulates NGF production in sympathetic target organs.

From a clinical perspective, ET_A receptor antagonists are known to improve the prognosis of heart failure by preventing cardiac remodeling and ventricular dysfunction (32). ET_A receptor antagonists also have an antiarrhythmic effect in pathological hearts, although the mechanism remains unclear (33). Neural remodel-

ing in sympathetic nerve sprouting results in ventricular tachyarrhythmia in diseased human hearts and in animal models (7, 8). In contrast, β -blocker therapy decreases the risk of sudden death secondary to ventricular tachyarrhythmia in ischemic heart disease or congestive heart failure. Given that ET-1 is strongly induced in the process of heart disease, the beneficial effects of ET_A receptor antagonists as antiarrhythmic agents may be related to the remodeling of the sympathetic nervous system that is mediated by the ET-1-NGF pathway. Further studies are needed to investigate whether ET-1 augmentation leads to an increase in NGF in the diseased heart.

In conclusion, these findings indicate that ET-1 regulates NGF expression in cardiomyocytes and plays a critical role in sympathetic innervation of the heart.

Acknowledgments

This study was supported in part by research grants from the Ministry of Education, Culture, Sports, Science and Technology, Japan, and Health Science Research Grants for Advanced Medical Technology from the Ministry of Health, Labor and Welfare, Japan.

Received for publication July 14, 2003, and accepted in revised form December 16, 2003.

Address correspondence to: Keiichi Fukuda, Institute for Advanced Cardiac Therapeutics, Keio University School of Medicine, 35 Shinanomachi, Shinjuku-ku, Tokyo 160-8582, Japan. Phone: 81-3-5363-3874; Fax: 81-3-5363-3875; E-mail: kfukuda@sc.itc.keio.ac.jp.

- Loring, J.F., and Erickson, C.A. 1987. Neural crest cell migratory pathways in the trunk of the chick embryo. *Dev. Biol.* **121**:220-236.
- Snider, W.D. 1994. Functions of the neurotrophins during nervous system development: what the knockouts are teaching us. *Cell.* **77**:627-638.
- Lockhart, S.T., Turrigiano, G.G., and Birren, S.J. 1997. Nerve growth factor modulates synaptic transmission between sympathetic neurons and cardiac myocytes. *J. Neurosci.* **17**:9573-9582.
- Heumann, R., Korsching, S., Scott, J., and Thoenen, H. 1984. Relationship between levels of nerve growth factor (NGF) and its messenger RNA in sympathetic ganglia and peripheral target tissues. *EMBO J.* **3**:3183-3189.
- Brennan, C., Rivas-Plata, K., and Landis, S.C. 1999. The p75 neurotrophin receptor influences NT-3 responsiveness of sympathetic neurons *in vivo*. *Nat. Neurosci.* **2**:699-705.
- Hassankhani, A., et al. 1995. Overexpression of NGF within the heart of transgenic mice causes hyperinnervation, cardiac enlargement, and hyperplasia of ectopic cells. *Dev. Biol.* **169**:309-321.
- Cao, J.M., et al. 2000. Relationship between regional cardiac hyperinnervation and ventricular arrhythmia. *Circulation.* **101**:1960-1969.
- Cao, J.M., et al. 2000. Nerve sprouting and sudden cardiac death. *Circ. Res.* **86**:816-821.
- Kanki, H., et al. 1999. Comparison of nerve growth factor mRNA expression in cardiac and skeletal muscle in streptozotocin-induced diabetic mice. *Life Sci.* **65**:2305-2313.
- Kaye, D.M., Vaddadi, G., Gruskin, S.L., Du, X.J., and Esler, M.D. 2000. Reduced myocardial nerve growth factor expression in human and experimental heart failure. *Circ. Res.* **86**:E80-E84.
- Kunihara, Y., et al. 1994. Elevated blood pressure and craniofacial abnormalities in mice deficient in endothelin-1. *Nature.* **368**:703-710.
- Kunihara, Y., et al. 1995. Aortic arch malformations and ventricular septal defect in mice deficient in endothelin-1. *J. Clin. Invest.* **96**:293-300.
- Clouthier, D.E., et al. 1998. Cranial and cardiac neural crest defects in endothelin-A receptor-deficient mice. *Development.* **125**:813-824.
- Sano, M., et al. 2000. Interleukin-6 family of cytokines mediate angiotensin II-induced cardiac hypertrophy in rodent cardiomyocytes. *J. Biol. Chem.* **275**:29717-29723.
- Akamatsu, W., et al. 1999. Mammalian ELAV-like neuronal RNA-binding proteins HuB and HuC promote neuronal development in both the central and the peripheral nervous systems. *Proc. Natl. Acad. Sci. U. S. A.* **96**:9885-9890.
- Nishida, M., et al. 2000. G alpha (i) and G alpha (o) are target proteins of reactive oxygen species. *Nature.* **408**:492-495.
- Zhan, Y., et al. 2003. Role of JNK, p38, and ERK in platelet-derived growth factor-induced vascular proliferation, migration, and gene expression. *Arterioscler. Thromb. Vasc. Biol.* **23**:795-801.
- Colangelo, A.M., Johnson, P.F., and Mocchetti, I. 1998. Beta-adrenergic receptor-induced activation of nerve growth factor gene transcription in rat cerebral cortex involves CCAAT/enhancer-binding protein delta. *Proc. Natl. Acad. Sci. U. S. A.* **95**:10920-10925.
- Kodama, H., et al. 2003. Selective involvement of p130Cas/Crk/Pyk2/c-Src in endothelin-1-induced JNK activation. *Hypertension.* **41**:1372-1379.
- Tanimoto, K., et al. 1994. Angiotensinogen-deficient mice with hypotension. *J. Biol. Chem.* **269**:31334-31337.
- Nishimura, Y., Iro, T., Hoe, K., and Saavedra, J.M. 2000. Chronic peripheral administration of the angiotensin II AT(1) receptor antagonist candesartan blocks brain AT(1) receptors. *Brain Res.* **871**:29-38.
- Hjemdahl, P. 1984. Catecholamine measurements by high-performance liquid chromatography. *Am. J. Physiol.* **247**:E13-E20.
- Kawasaki, T., et al. 2002. Requirement of neuropilin 1-mediated Sema3A signals in patterning of the sympathetic nervous system. *Development.* **129**:671-680.
- Francis, N., et al. 1999. NT-3, like NGF, is required for survival of sympathetic neurons, but not their precursors. *Dev. Biol.* **210**:411-427.
- Selby, M.J., Edwards, R., Sharp, F., and Rutter, W.J. 1987. Mouse nerve growth factor gene: structure and expression. *Mol. Cell. Biol.* **7**:3057-3064.
- Chiloeches, A., et al. 1999. Regulation of Ras. GTP loading and Ras-Raf association in neonatal rat ventricular myocytes by G protein-coupled receptor agonists and phorbol ester. Activation of the extracellular signal-regulated kinase cascade by phorbol ester is mediated by Ras. *J. Biol. Chem.* **274**:19762-19770.
- Sugden, P.H., and Clerk, A. 1997. Regulation of the ERK subgroup of MAP kinase cascades through G protein-coupled receptors. *Cell. Signal.* **9**:337-351.
- Story, G.M., et al. 2000. Inactivation of one copy of the mouse neurotrophin-3 gene induces cardiac sympathetic deficits. *Physiol. Genomics.* **27**:129-136.
- Zou, Y., et al. 1998. Cell type-specific angiotensin II-evoked signal transduction pathways. *Circ. Res.* **82**:337-345.
- Mocchetti, I., et al. 1989. Regulation of nerve growth factor biosynthesis by beta-adrenergic receptor activation in astrocytoma cells: a potential role of c-Fos protein. *Proc. Natl. Acad. Sci. U. S. A.* **86**:3891-3895.
- Clegg, D.O., Large, T.H., Bodary, S.C., and Reichardt, L.F. 1989. Regulation of nerve growth factor mRNA levels in developing rat heart ventricle is not altered by sympathectomy. *Dev. Biol.* **134**:30-37.
- Sakai, S., et al. 1996. Inhibition of myocardial endothelin pathway improves long-term survival in heart failure. *Nature.* **384**:353-355.
- Matsumoto, Y., et al. 2002. Long-term endothelin 1 receptor blockade inhibits electrical remodeling in cardiomyopathic hamsters. *Circulation.* **106**:613-619.

Leukemia Inhibitory Factor Activates Cardiac L-Type Ca^{2+} Channels via Phosphorylation of Serine 1829 in the Rabbit $\text{Ca}_v1.2$ Subunit

Eiichi Takahashi, Keiichi Fukuda, Shunichiro Miyoshi, Mitsushige Murata, Takahiro Kato, Makoto Ita, Tsutomu Tanabe, Satoshi Ogawa

Abstract—We have previously reported that leukemia inhibitory factor (LIF) gradually increased cardiac L-type Ca^{2+} channel current (I_{CaL}), which peaked at 15 minutes in both adult and neonatal rat cardiomyocytes, and this increase was blocked by the mitogen-activated protein kinase kinase inhibitor PD98059. This study investigated the molecular basis of LIF-induced augmentation of I_{CaL} in rodent cardiomyocytes. LIF induced phosphorylation of a serine residue in the α_{1c} subunit ($\text{Ca}_v1.2$) of L-type Ca^{2+} channels in cultured rat cardiomyocytes, and this phosphorylation was inhibited by PD98059. When constructs encoding either a wild-type or a carboxyl-terminal-truncated rabbit $\text{Ca}_v1.2$ subunit were transfected into HEK293 cells, LIF induced phosphorylation of the resultant wild-type protein but not the mutant protein. Cotransfection of constitutively active mitogen-activated protein kinase kinase also resulted in phosphorylation of the $\text{Ca}_v1.2$ subunit in the absence of LIF stimulation. In in-gel kinase assays, extracellular signal-regulated kinase phosphorylated a glutathione *S*-transferase fusion protein of the carboxyl-terminal region of $\text{Ca}_v1.2$ (residues 1700 through 1923), which contains the consensus sequence Pro-Leu-Ser-Pro. A point mutation within this consensus sequence, which results in a substitution of alanine for serine at residue 1829 (S1829A), was sufficient to abolish the LIF-induced phosphorylation. LIF increased I_{CaL} in HEK cells transfected with wild-type $\text{Ca}_v1.2$ but not with the mutated version. These results provide direct evidence that LIF phosphorylates the serine residue at position 1829 of the $\text{Ca}_v1.2$ subunit via the actions of extracellular signal-regulated kinase and that this phosphorylation increases I_{CaL} in cardiomyocytes. (*Circ Res.* 2004;94:1242-1248.)

Key Words: cardiomyocytes ■ extracellular signal-regulated kinase ■ leukemia inhibitory factor ■ L-type Ca^{2+} channels ■ phosphorylation

The cardiac L-type Ca^{2+} channel is the predominant ion channel within the heart, with each cardiomyocyte expressing $\sim 30\,000$ copies.¹ Cardiac L-type Ca^{2+} channels play essential roles in cardiac excitability, in coupling excitation to contraction, and in arrhythmogenesis. The channel is composed of four subunits, α_1 , α_2 , β_2 , and δ , and some channel functions are regulated by phosphorylation of the α_{1c} subunit ($\text{Ca}_v1.2$).² Protein kinase A (PKA) has been shown to phosphorylate the serine residue at the carboxyl end of $\text{Ca}_v1.2$,^{3,4} and protein kinase C (PKC) may phosphorylate $\text{Ca}_v1.2$ at the amino terminal.⁵ These findings suggest that phosphorylation of the intracellular domain of the cardiac L-type Ca^{2+} channel may be the critical mechanism for modulating its current.

Leukemia inhibitory factor (LIF) is a member of the interleukin-6 family and has a potent hypertrophic effect on cardiomyocytes.⁶ We and others have demonstrated that

JAK/STAT,^{6,7} mitogen-activated protein kinase,⁸ phosphatidylinositol 3 kinase,⁹ and calmodulin-dependent kinase¹⁰ lie downstream of gp130 in cardiomyocytes and that these pathways play important roles in mediating cardiac hypertrophy. While investigating the molecular mechanism of LIF-induced cardiac hypertrophy, we found that this cytokine increases the L-type Ca^{2+} current (I_{CaL}) in cardiomyocytes.¹¹ Although the molecular mechanisms by which LIF stimulates I_{CaL} remains unknown, we have shown it to be independent of PKA and PKC and have shown that the mitogen-activated protein kinase kinase (MEK) inhibitor PD98059 specifically inhibits the LIF-induced amplification of I_{CaL} . We also identified two extracellular signal-regulated kinase (ERK) consensus sequences (Pro-X-Ser and Thr-Pro) at the carboxyl end of $\text{Ca}_v1.2$ and showed that they are conserved among different species (human, rat, mouse, and rabbit). Based on

Original received June 10, 2003; resubmission received November 6, 2003; revised resubmission received March 11, 2004; accepted March 11, 2004. From the Institute for Advanced Cardiac Therapeutics (E.T., K.F., S.M.), Cardiopulmonary Division, Department of Internal Medicine (M.M., T.K., S.O.), and Pharmacia-Keio Research Laboratories (M.I.), Shinanomachi Research Park, Keio University School of Medicine, and Department of Pharmacology and Neurobiology (T.T.), Graduate School of Medicine, Tokyo Medical and Dental University, Core Research for Evolutional Science and Technology, Japan Science and Technology Corporation, Tokyo, Japan.

This manuscript was sent to Stephen F. Vatner, Consulting Editor, for review by expert referees, editorial decision, and final deposition.

Correspondence to Keiichi Fukuda, MD, PhD, Institute for Advanced Cardiac Therapeutics, Keio University School of Medicine, 35 Shinanomachi, Shinjuku-ku, Tokyo 160-8582, Japan. E-mail kfukuda@sc.itc.keio.ac.jp

© 2004 American Heart Association, Inc.

Circulation Research is available at <http://www.circresaha.org>

DOI: 10.1161/01.RES.0000126405.38858.BC

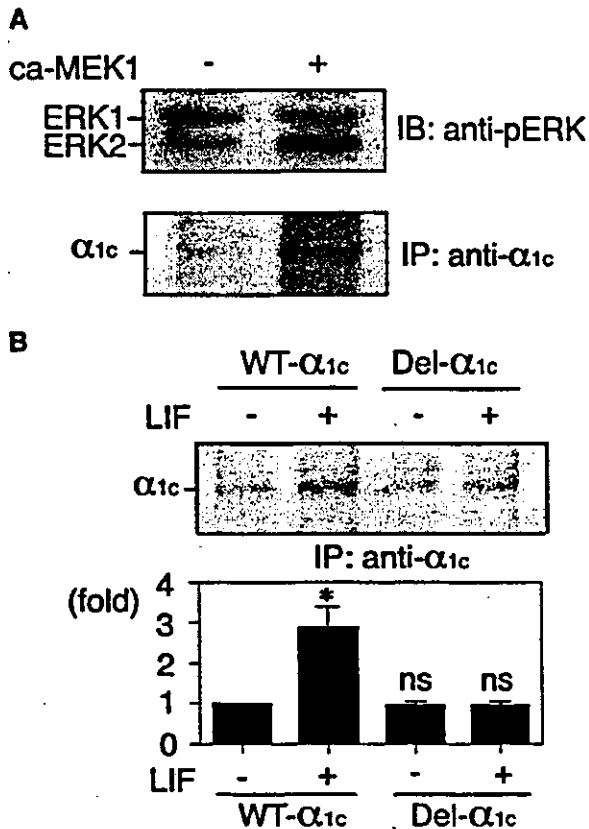


Figure 4. LIF phosphorylates the $\text{Ca}_v1.2$ subunit of the L-type Ca^{2+} channel in vitro at the carboxyl terminal via the MEK/ERK pathway. **A**, Wild-type- $\text{Ca}_v1.2$ was cotransfected with constitutive active MEK1 (caMEK1) and β_{2b} subunit, and phosphorylation of $\text{Ca}_v1.2$ was detected. The caMEK1-transfected cells showed phosphorylation of $\text{Ca}_v1.2$ in the absence of LIF stimulation, indicating that the MEK1/ERK1 pathway was sufficient to induce phosphorylation. A representative autoradiogram from 4 independent experiments is shown. **B**, Wild-type (WT) or a deletion mutant (Del) lacking the carboxyl terminal of $\text{Ca}_v1.2$ was transfected into HEK293 cells with the β_{2b} subunit, and the cells were stimulated with LIF. The wild-type $\text{Ca}_v1.2$ was phosphorylated with LIF, but the deletion mutant was unaffected by LIF. Results were the mean of 5 separate experiments, in which each experiment showed similar results. ns indicates not significant vs control [LIF(-), PD98059(-)], * $P < 0.05$ vs control.

with LIF. Although the wild-type $\text{Ca}_v1.2$ was phosphorylated 2.9-fold greater than the control ($n = 5$, $P < 0.05$), the deletion mutant was not phosphorylated by LIF at all ($n = 5$, not significant) (Figure 4B).

LIF Phosphorylates the Carboxyl-Terminal of $\text{Ca}_v1.2$ From Amino Acids 1812 through 2171

To identify the phosphorylation site, we prepared deleted GST-fusion proteins of $\text{Ca}_v1.2$ as a substrate and performed in-gel kinase assays. The three deleted fusion proteins contained either no ERK1/2 consensus sequences, the Pro-Leu-Ser-Pro sequence, or the Pro-Ala-Thr-Pro sequence (see also Figure 1). Serum-starved primary cultured rat neonatal cardiomyocytes and rat aortic smooth muscle cells were incubated for 15 minutes with LIF and angiotensin II, respectively, and in-gel kinase assays were performed using myelin basic protein (MBP), GST, or deleted $\text{Ca}_v1.2$ GST-fusion

proteins. ERK1/2, which was activated by LIF, phosphorylated the MBP and the protein containing the Pro-Leu-Ser-Pro consensus sequence, and this phosphorylation was blocked by preincubation with PD98059 (Figure 5). These findings indicate that activated ERK1/2 can phosphorylate the carboxyl terminal of $\text{Ca}_v1.2$ between amino acids 1700 and 1923.

$\text{Ca}_v1.2$ Is Specifically Phosphorylated by LIF at Serine 1829

To confirm that the LIF-induced phosphorylation of the carboxyl-terminal of the L-type Ca^{2+} channel actually occurred at the ERK target sequence (Pro-Leu-Ser-Pro, 1827 through 1830), we cotransfected HEK293 cells with the β_{2b} subunit and constructs encoding either the S1829A mutant $\text{Ca}_v1.2$ or wild-type $\text{Ca}_v1.2$. Cells were then metabolically labeled with ^{32}P -orthophosphate. After treatment with LIF, the wild-type $\text{Ca}_v1.2$ was phosphorylated 2.9-fold over the control, whereas the mutant $\text{Ca}_v1.2$ remained unphosphorylated (Figure 6), indicating that $\text{Ca}_v1.2$ was specifically phosphorylated at serine 1829.

LIF Increased I_{CaL} in the Wild-Type $\text{Ca}_v1.2$ but not in the S1829A Mutant $\text{Ca}_v1.2$

To confirm that the S1829A point mutation in $\text{Ca}_v1.2$ abolished the response to LIF, we measured the peak inward current in HEK293 cells cotransfected with the β_{2b} subunit and either wild-type or mutant $\text{Ca}_v1.2$. In our preliminary conventional whole-cell patch clamp experiment, the peak inward current varied from 0 to 6 nA in wild-type ($n = 57$) and from 0 to 2 nA in mutant ($n = 30$) cells, but the difference was not statistically significant. Little or no inward current (< 50 pA) was observed in 10 GFP-positive wild-type cells or in four GFP-positive mutant cells. Although some cells displayed large currents (> 1 nA; $n = 2$ in wild-type, $n = 1$ in mutant), the current density was generally similar between the two groups. In the perforation patch-clamp experiment, the amplitude of the current was stable during the observation period, suggesting no natural run down. The amplitude of the peak current 5 minutes after exposure to LIF increased in the wild-type $\text{Ca}_v1.2$ cells ($38 \pm 40\%$, $n = 7$), whereas there was a small decrease in current in mutant cells ($-16 \pm 10\%$, $n = 7$, $P < 0.05$ versus wild-type). A representative time course of the increase in I_{CaL} is shown in Figure 7. The representative original current trace was shown in online Figures 1 and 2 (available in the online data supplement at <http://circres.ahajournals.org>). Cells transfected with wild-type showed an increase in the amplitude of the current 5 minutes after exposure to LIF that reached a maximum after 20 minutes. Cells transfected with mutant showed a small decrease immediately after the change of solution that was stable for > 30 minutes. Furthermore, extracellular application of 10 $\mu\text{mol/L}$ dB-cAMP or 8Br-cAMP did not increase the I_{CaL} in wild-type cells, suggesting there is no PKA pathway to phosphorylate the L-type Ca^{2+} channel in HEK293 cells (data not shown). These results indicated that the LIF-induced increase in I_{CaL} was mediated by the phosphorylation of serine 1829.

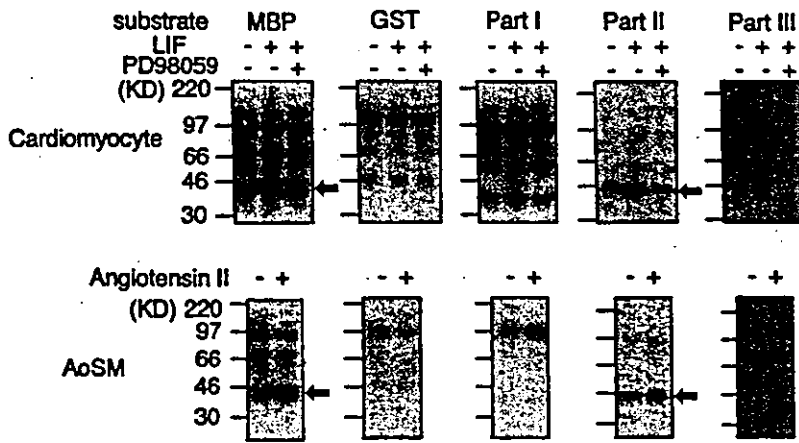


Figure 5. LIF phosphorylated the Ca_v1.2 subunit of the L-type Ca²⁺ channel in vitro at the carboxyl terminal from positions 1700 through 1923 via the MEK/ERK pathway. GST-fusion proteins were prepared for 3 regions of the carboxyl terminal of Ca_v1.2. Part I, 1472 through 1699; part II, 1700 through 1923; and part III, 1924 through 2171. In-gel phosphorylation of the GST-fusion proteins was assessed by using LIF-stimulated cardiomyocyte lysates (top) or angiotensin II-stimulated RASM cell lysates (bottom). Arrows indicate that 42- and 44-kDa ERK1/2 phosphorylated the substrates (MBP and part I). A representative autoradiogram from 3 independent experiments is shown.

Discussion

This study investigated the molecular mechanisms of the LIF-induced increase in I_{CaL}. LIF was found to induce specific phosphorylation of serine 1829 of rabbit Ca_v1.2, the α_{1c} subunit of the cardiac L-type Ca²⁺ channel. Because LIF failed to induce any increase in current when the subunit contained an S1829A point mutation, we have shown that this phosphorylation event is necessary for the observed increase in I_{CaL}. The serine residue at position 1829 lies within an

ERK1/2 consensus phosphorylation sequence and is therefore phosphorylated either by ERK1/2 or kinases activated by ERK1/2. In agreement with a previous study,²³ PKA activation by the cell-permeable cAMP compound failed to increase I_{CaL} in HEK293 cells because of the lack of A-kinase anchoring protein. This also suggests that the LIF-induced increase in I_{CaL} in this system follows a pathway independent of the PKA pathway.

Ca_v1.2, which is critical for the modulation of the I_{CaL}, is regulated via phosphorylation by various kinases at different positions in the intracellular domains, especially the long carboxyl-terminal domain. De Jongh et al⁵ showed that PKA phosphorylates the serine residue at position 1928 of the carboxyl terminal of Ca_v1.2 and that this phosphorylation enhances cellular Ca²⁺ entry in response to β-adrenergic receptor stimulation. Leach et al²⁴ reported that PKA also phosphorylates serine 1627 and serine 1700 in the carboxyl terminal of Ca_v1.2 in response to β-adrenergic stimulation. These findings suggest that PKA-activating pathways modulate the I_{CaL} in cardiac muscle and that the C-terminal of Ca_v1.2 is a substrate for PKA. Shistik et al⁵ demonstrated that PKC inhibits I_{CaL} by phosphorylating threonine 27 and threonine 31 at the N-terminal of Ca_v1.2, whereas Jiang et al²⁵ reported that cGMP inhibits I_{CaL} by phosphorylating serine 533 of Ca_v1.2 via the action of protein kinase G. Recent studies have revealed that the β subunit of the L-type Ca²⁺ channel also plays an important role in modulating the I_{CaL}. Haase and colleagues^{26,27} reported that PKA phosphorylates the β subunit and increases Ca²⁺ entry in response to β-adrenergic stimulation both in vivo and in vitro. Bünnemann et al²⁸ showed that phosphorylation of serine 478 and serine 479 of the β₂ subunit is involved in this PKA-dependent augmentation of I_{CaL}.

This study has identified a novel regulatory mechanism of cardiac I_{CaL}. To our knowledge, this is the first report of ERK1/2 involvement in the regulation of cardiac I_{CaL}. There seem to be several reasons why this involvement has not been previously recognized. After ligand stimulation, PKA, PKC, and protein kinase G are rapidly activated following the rapid increase of the upstream second messengers cAMP, DG, and cGMP. As a result, these kinases can phosphorylate Ca_v1.2 and modulate the I_{CaL} at an early stage, eg, 1 to 5 minutes after the stimulus. By contrast, ERK1/2 is activated through

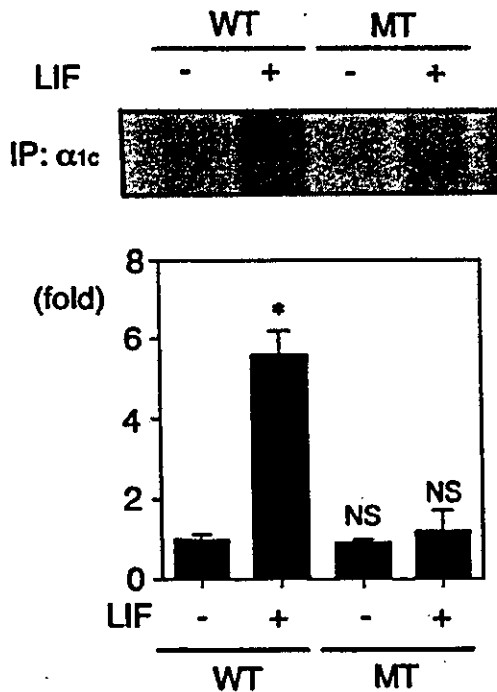


Figure 6. Ca_v1.2 is specifically phosphorylated by LIF at serine 1829. Wild-type Ca_v1.2 (WT) or the point mutant Ca_v1.2 (serine 1829 to alanine substitution, MT) was transfected together with the β_{2b} subunit into HEK293 cells and metabolically labeled with ortho-³²P. Cells were stimulated with LIF for 15 minutes, and the wild-type or mutant Ca_v1.2 was immunoprecipitated. The increased intensity of the phosphorylation of the Ca_v1.2 was normalized by the intensity of the phosphorylation in the absence of LIF stimulation in wild-type and mutant cells, respectively. Results are the mean of 3 separate experiments, in which each experiment showed similar results. ns indicates not significant vs control [LIF(-), PD98059(-)], *P<0.05 vs control.

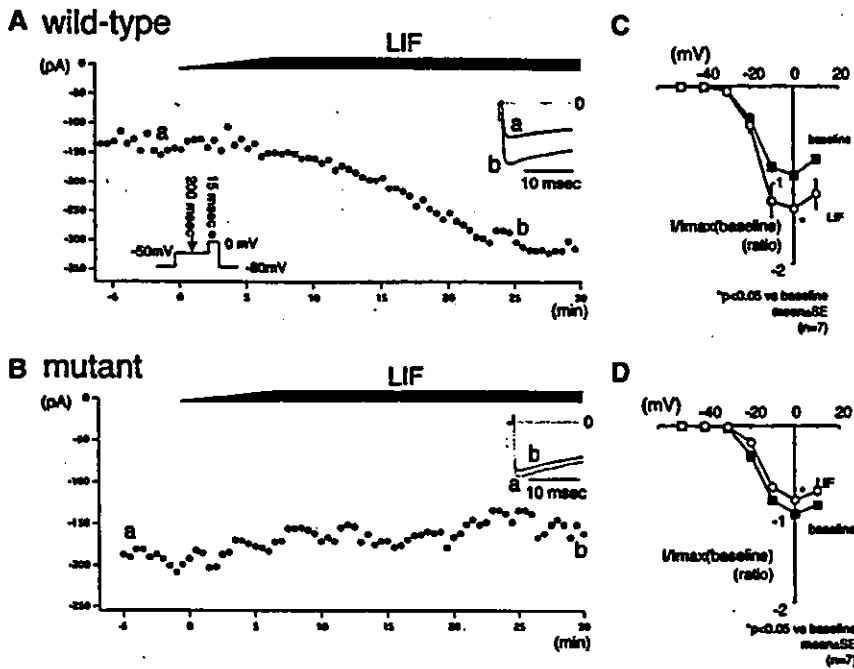


Figure 7. LIF increased I_{CaL} in the wild-type $\text{Ca}_v1.2$ but not in the S1829A mutant $\text{Ca}_v1.2$. The function of the transfected L-type Ca^{2+} channels was analyzed by gramicidin-perforated patch clamping. Time courses of I_{CaL} for transfected L-type Ca^{2+} channels (wild-type [A] and mutant [B]) in HEK293 cells are shown. The points in the figures are peak inward current amplitudes at 0 mV every 10 seconds. Voltage protocol is shown in the inset. Solid bar at the top of the figure indicates the duration of exposure to LIF. Current trace for each time point was superimposed for each corresponding symbol and is shown as an inset in the top right corner. Current amplitude peaked at ~20 to 25 minutes in wild-type L-type Ca^{2+} channels but did not increase or show a natural rundown in mutant L-type Ca^{2+} channels. Amplitude of inward currents before (baseline) and after LIF administration was normalized to the maximal inward current at the baseline. Averaged data are plotted against the test membrane potential in right panels (wild-type [C] and mutant [D]). LIF increased the I_{CaL} only in wild-type L-type Ca^{2+} channels, without changing the current-voltage relationship. Mutant L-type Ca^{2+} channels were unaffected.

various signaling molecules, such as sos, shc, Grb2, raf1, and MEK, and its activation does not peak until 8 to 15 minutes after the stimulus. The activation by LIF peaked at 15 minutes. In addition, the ERK-mediated increase in I_{CaL} was only ~25% to 30% greater than baseline, far smaller than the increase by PKA. Presumably, this relatively small and slow increase in Ca^{2+} current caused by ERK or its downstream kinases was easily masked by the other stimuli. For example, endothelin-1 is known to increase I_{CaL} in cardiomyocytes. Because the ET-A receptor is linked to $\text{G}_\beta/\text{G}_\gamma/\text{G}_q$, endothelin-1 stimulation rapidly increases cAMP and IP₃, resulting in rapid activation of PKA and PKC at as early as 1 to 3 minutes.^{29,30} Endothelin-1 also activates ERK, but its activation peaks at 8 to 10 minutes,³¹ and thus the rapid activation of PKA or PKC may mask the ERK-mediated augmentation of I_{CaL} by endothelin-1. By contrast, the signaling pathway via LIF uses raf1/MEK/ERK, JAK/STAT, and phosphatidylinositol 3-kinase/AKT pathways through gp130 and not the PKA or PKC pathways. Presumably we were able to detect ERK1/2-mediated modification of cardiac L-type Ca^{2+} channels because LIF activates ERK and not PKA or PKC.

ERK1/2 is a ubiquitously expressed member of the mitogen-activated protein kinase family, which is activated in response to a variety of extracellular stimuli. It has been implicated in both growth and apoptosis in the cardiovascular system. The downstream substrates of ERK include other kinases, transcription factors, and membrane receptors and other cell mediators. The only evidence of ERK functioning in the regulation of the activity of membrane ion channels has come from neurological studies. Adams and colleagues^{32,33} reported that the A-type potassium channel K_v4.2 is a substrate for ERK in hippocampal neurons and demonstrated that ERK phosphorylates threonine 602, threonine 607, and serine 616 within the cytoplasmic domain. Shi et al³⁴ demonstrated that ERK phosphorylates the carboxyl terminal of

the β (threonine 613) and γ (threonine 623) subunits of the epithelial Na^+ channel, thereby facilitating their interactions with the ubiquitin ligase Nedd4, which ultimately inhibits channel activity. These findings indicate that the phosphorylation of membrane ion channels by ERK1/2 is perhaps not an uncommon regulatory mechanism. This study is the first to demonstrate involvement of ERK1/2 in modifying cardiac ion channels.

In the present study, the phosphorylation status of the β_{2b} subunit was not investigated, because preliminary experiments showed that LIF does not cause phosphorylation of this subunit. Our finding that the point mutation of $\text{Ca}_v1.2$ at serine 1829 completely abolishes the increase in I_{CaL} suggests that it is unlikely that phosphorylation of the β_{2b} subunit plays a critical role in the regulation of the LIF-induced increase in I_{CaL} . Because cardiac L-type Ca^{2+} channels are critical ion channels in the control of cardiac function, additional investigations are needed to precisely identify all of the regulatory mechanisms involved.

Acknowledgments

This study was supported in part by research grants from the Ministry of Education, Science and Culture, Japan (to K.F. and E.T.), the Health Science Research Grants for Advanced Medical Technology from the Ministry of Welfare, Japan (to K.F.), the Japan Heart Foundation (Molecular Cardiology Fund by Zeria New Drug Inc) (to E.T.), and the Takeda Science Foundation (to E.T.). We also thank Haruko Kawaguchi and Yasuyo Hisaka for their technical help.

References

- Rose WC, Balke CW, Wier WG, Marbán E. Macroscopic and unitary properties of physiological ion flux through L-type Ca channels in guinea pig heart cells. *J Physiol.* 1992;456:267-284.
- Kamp TJ, Hell JW. Regulation of cardiac L-type calcium channels by protein kinase A and protein kinase C. *Circ Res.* 2000;87:1095-1102.
- De Jongh KS, Murphy BJ, Colvin AA, Hell JW, Takahashi M, Catterall WA. Specific phosphorylation of a site in the full-length form of the α_1 subunit of the cardiac L-type calcium channel by adenosine 3',5'-cyclic

- monophosphate-dependent protein kinase. *Biochemistry*. 1996;35:10392-10402.
4. Perets T, Blumenstein Y, Shistik E, Lotan I, Dascal N. A potential site of functional modulation by protein kinase A in the cardiac Ca^{2+} channel $\alpha_1\text{C}$ subunit. *FEBS Lett*. 1996;384:189-192.
 5. Shistik E, Ivanina T, Blumenstein Y, Dascal N. Crucial role of the N terminus in function of cardiac L-type Ca^{2+} channel and its modulation by protein kinase C. *J Biol Chem*. 1998;273:17901-17909.
 6. Kodama H, Fukuda K, Pan J, Makino S, Baba A, Hori S, Ogawa S. Leukemia inhibitory factor, a potent cardiac hypertrophic cytokine, activates the JAK/STAT pathway in rat cardiomyocytes. *Circ Res*. 1997;81:656-663.
 7. Kunisada K, Hirota H, Fujio Y, Matsui H, Tani Y, Yamauchi-Takahara K, Kishimoto T. Activation of JAK-STAT and MAP kinases by leukemia inhibitory factor through gp130 in cardiac myocytes. *Circulation*. 1996;94:2626-2632.
 8. Kodama H, Fukuda K, Pan J, Sano M, Takahashi T, Kato T, Makino S, Manabe T, Murata M, Ogawa S. Significance of Raf-1/MEK/ERK cascade compared with JAK/STAT and PI3-K pathways in gp130-mediated cardiac hypertrophy. *Am J Physiol*. 2000;279:H1635-H1644.
 9. Oh H, Fujio Y, Kunisada K, Hirota H, Matsui H, Kishimoto T, Yamauchi-Takahara K. Activation of phosphatidylinositol 3-kinase through glycoprotein 130 induces protein kinase B and p70 S6 kinase phosphorylation in cardiac myocytes. *J Biol Chem*. 1998;273:9703-9710.
 10. Kato T, Sano M, Miyoshi S, Sato T, Hakuno D, Ishida H, Nakazawa H, Fukuda K, Ogawa S. Calmodulin kinases II and IV and calcineurin are involved in leukemia inhibitory factor-induced cardiac hypertrophy in rats. *Circ Res*. 2000;87:937-945.
 11. Murata M, Fukuda K, Ishida H, Miyoshi S, Koura T, Kodama H, Nakazawa HK, Ogawa S. Leukemia inhibitory factor, a potent cardiac hypertrophic cytokine, enhances L-type Ca^{2+} current and $[\text{Ca}^{2+}]_i$ transient in cardiomyocytes. *J Mol Cell Cardiol*. 1999;31:237-245.
 12. Pan J, Fukuda K, Kodama H, Makino S, Takahashi T, Sano M, Hori S, Ogawa S. Role of angiotensin II in activation of the JAK/STAT pathway induced by acute pressure-overload in the rat heart. *Circ Res*. 1997;81:611-617.
 13. Takahashi E, Abe J, Berk BC. Angiotensin II stimulates p90rsk in vascular smooth muscle cells: a potential Na^+/H^+ exchanger kinase. *Circ Res*. 1997;81:268-273.
 14. Takahashi E, Abe J, Gallis B, Aebersold R, Spring DJ, Krebs EG, Berk BC. p90rsk is a serum-stimulated NHE1 kinase: regulatory phosphorylation of serine 703 of Na^+/H^+ exchanger isoform-1. *J Biol Chem*. 1999;274:20206-20214.
 15. Mikami A, Imoto K, Tanabe T, Niidome T, Mori Y, Takeshima H, Narumiya S, Numa S. Primary structure and functional expression of the cardiac dihydropyridine-sensitive calcium channel. *Nature*. 1989;340:230-233.
 16. Gallis B, Corthals GL, Goodlet DR, Ueba H, Kim F, Presnell SR, Figeys D, Harrison DG, Berk BC, Aebersold R, Corson MA. Identification of flow-dependent endothelial nitric-oxide synthase phosphorylation sites by mass spectrometry and regulation of phosphorylation and nitric oxide production by the phosphatidylinositol 3-kinase inhibitor LY294002. *J Biol Chem*. 1999;274:30101-30108.
 17. Tateyama M, Zong S, Tanabe T, Ochi R. Properties of $\alpha_{1\text{C}}$ Ca^{2+} channel currents expressed in cultured adult rabbit ventricular myocytes. *Am J Physiol Cell Physiol*. 2001;280:C175-C182.
 18. Kawamura A, Gordon MW. Perforated-patch recording does not enhance effect of 3-isobutyl-1-methylxanthine on cardiac calcium current. *Am J Physiol*. 1994;266:C1619-C1627.
 19. Akaike N, Harata N. Nystatin perforated patch recording and its application to analysis of intracellular mechanisms. *Jpn J Physiol*. 1994;44:433-473.
 20. Varadi G, Schwartz A. Cloning, chromosomal localization, and functional expression of the α_1 subunit of the L-type voltage-dependent calcium channel from normal human heart. *Proc Natl Acad Sci USA*. 1993;90:6228-6232.
 21. Slish DF, Engle DB, Varadi G, Lotan I, Singer D, Dascal N, Schwartz A. Evidence for the existence of a cardiac specific isoform of the α_1 subunit of the voltage dependent calcium channel. *FEBS Lett*. 1989;250:509-514.
 22. Gotoh Y, Matsuda S, Takenaka K, Hattori S, Iwamatsu A, Ishikawa M, Kosako H, Nishida E. Characterization of recombinant *Xenopus* MAP kinase kinases mutated at potential phosphorylation sites. *Oncogene*. 1994;9:1891-1898.
 23. Iain DCF, Steven JT, Linda BL, Lorene KL, Ann MW, Rebecca AD, Neil VM, John DS. A novel lipid-anchored A-kinase anchoring protein facilitates cAMP-responsive membrane events. *EMBO J*. 1998;17:2261-2272.
 24. Leach RN, Brickley K, Norman RI. Cyclic AMP-dependent protein kinase phosphorylates residues in the C-terminal domain of the cardiac L-type calcium channel α_1 subunit. *Biochim Biophys Acta*. 1996;1281:205-212.
 25. Jiang LH, Gawler DJ, Hodson N, Milligan CJ, Pearson HA, Porter V, Wray D. Regulation of cloned cardiac L-type calcium channels by cGMP-dependent protein kinase. *J Biol Chem*. 2000;275:6135-6143.
 26. Haase H, Karczewski P, Beckert R, Krause EG. Phosphorylation of the L-type calcium channel β subunit is involved in β -adrenergic signal transduction in canine myocardium. *FEBS Lett*. 1993;335:217-222.
 27. Haase H, Bartel S, Karczewski P, Morano I, Krause EG. In-vivo phosphorylation of the cardiac L-type calcium channel β -subunit in response to catecholamines. *Mol Cell Biochem*. 1996;163-164:99-106.
 28. Bünemann M, Gerhardstein BL, Gao T, Hosey MM. Functional regulation of L-type calcium channels via protein kinase A-mediated phosphorylation of the β_2 subunit. *J Biol Chem*. 1999;274:33851-33854.
 29. Rebsamen MC, Church DJ, Morabito D, Vallotton MB, Lang U. Role of cAMP and calcium influx in endothelin-1-induced ANP release in rat cardiomyocytes. *Am J Physiol*. 1997;273:E922-E931.
 30. Takanashi M, Endoh M. Concentration- and time-dependence of phosphoinositide hydrolysis induced by endothelin-1 in relation to the positive inotropic effect in the rabbit ventricular myocardium. *J Pharmacol Exp Ther*. 1992;262:1189-1194.
 31. Yue TL, Gu JL, Wang C, Reith AD, Lee JC, Mirabile RC, Kreutz R, Wang Y, Maleeff B, Parsons AA, Ohlstein EH. Extracellular signal-regulated kinase plays an essential role in hypertrophic agonists, endothelin-1 and phenylephrine-induced cardiomyocyte hypertrophy. *J Biol Chem*. 2000;275:37895-37901.
 32. Adams JP, Anderson AE, Varga AW, Dineley KT, Cook RG, Pfaffinger PJ, Sweatt JD. The A-type potassium channel Kv4.2 is a substrate for the mitogen-activated protein kinase ERK. *J Neurochem*. 2000;75:2277-2287.
 32. Yuan LL, Adams JP, Swank M, Sweatt JD, Johnston D. Protein kinase modulation of dendritic K^+ channels in hippocampus involves a mitogen-activated protein kinase pathway. *J Neurosci*. 2002;22:4860-4868.
 33. Yuan LL, Adams JP, Swank M, Johnston D. Protein kinase modulation of dendritic K^+ channels in hippocampus involves a mitogen-activated protein kinase pathway. *J Neurosci*. 2002;22:4860-4868.
 34. Shi H, Asher C, Chigaev A, Yung Y, Reuveny E, Seger R, Garty H. Interactions of β and γ ENaC with Nedd4 can be facilitated by an ERK-mediated phosphorylation. *J Biol Chem*. 2002;277:13539-13547.

Purified cardiomyocytes from bone marrow mesenchymal stem cells produce stable intracardiac grafts in mice

Naoichiro Hattan^{a,1}, Haruko Kawaguchi^{b,1}, Kiyoshi Ando^c, Eriko Kuwabara^a, Jun Fujita^d,
Mitsushige Murata^d, Makoto Suematsu^b, Hidezo Mori^a, Keiichi Fukuda^{d,*}

^aDepartment of Physiology, Tokai University School of Medicine, Japan

^bDepartment of Biochemistry and Integrative Medical Biology, Keio University School of Medicine, Tokyo, Japan

^cDepartment of Hematology and Oncology, Tokai University School of Medicine, Japan

^dDepartment of Medicine, Division of Cardiology, Keio University School of Medicine, 35 Shinanomachi, Shinjuku-ku, Tokyo 160-8582, Japan

Received 16 April 2004; received in revised form 4 October 2004; accepted 5 October 2004

Available online 28 October 2004

Time for primary review 21 days

Abstract

Objective: We have previously isolated cardiomyogenic cells from murine bone marrow (CMG cells). Regenerated cardiomyocytes are important candidates for cell transplantation, but as they are stem cell derived, they can be contaminated with various cell types, thereby requiring characterization and purification. Our objectives were to increase the efficiency of cell transplantation and to protect the recipients from possible adverse effects using an efficient and effective purification process as well as to characterize regenerated cardiomyocytes.

Methods: Noncardiomyocytes were eliminated from a mixture of stem-cell-derived cells using a fluorescence-activated cell sorter to specifically isolate CMG cells transfected with a recombinant plasmid containing enhanced green fluorescent protein (EGFP) cDNA under the control of the myosin light chain-2v (MLC-2v) promoter. Gene expression and the action potential were investigated, and purified cells were transplanted into the heart of adult mice.

Results: Six percent to 24% of transfected CMG cells expressed EGFP after differentiation was induced, and a strong EGFP-positive fraction was selected. All the sorted cells began spontaneous beating after 3 weeks. These cells expressed cardiomyocyte-specific genes such as α -skeletal actin, β -myosin heavy chain, MLC-2v, and CaV1.2 and incorporated bromodeoxyuridine for 5 days. The isolated EGFP-positive cells were expanded for 5 days and then transplanted into the left ventricle of adult mouse hearts. The transplanted cells survived for at least 3 months and were oriented in parallel to the cardiomyocytes of the recipient heart.

Conclusions: The purification and transplantation of differentiated cardiomyocytes from adult stem cells provides a viable model of tissue engineering for the treatment of heart failure.

© 2004 European Society of Cardiology. Published by Elsevier B.V. All rights reserved.

Keywords: Cardiomyocytes; Heart failure; Transplantation; Stem cell; Bone marrow

This article is referred to in the Editorial by B. Dawn and R. Bolli (pages 293–295) in this issue.

1. Introduction

Necrotic cardiomyocytes in infarcted ventricular tissue are progressively replaced by fibroblasts leading to the formation of scar tissue and this loss of cardiomyocytes leads to regional contractile dysfunction. Transplanted fetal cardiomyocytes can survive in heart scar tissue, thereby limiting scar expansion and preventing post-infarction heart failure [1–3]. The transplantation of cultured cardiomyocytes into damaged myocardium has been proposed as a novel method

* Corresponding author. Tel.: +81 3 5363 3874; fax: +81 3 5363 3875.

E-mail address: kfukuda@sc.itc.keio.ac.jp (K. Fukuda).

¹ Naoichiro Hattan and Haruko Kawaguchi contributed equally to this paper.

for treating heart failure. While this is a revolutionary idea, it remains clinically unfeasible due to the difficulty in obtaining donor fetal hearts. For this reason, research has focused on the development of a cardiomyogenic cell line to treat heart failure by transplantation therapy.

Advances in regenerative medicine have enabled the generation of various cell types from embryonic stem (ES) cells or adult stem cells [4,5]. We recently reported the generation of cardiomyocytes from marrow mesenchymal stem cells *in vitro* (CMG cells) and demonstrated that these cells spontaneously beat, express atrial natriuretic factors, and possess a fetal ventricular cardiomyocyte-like phenotype [6]. We also reported that cardiomyocytes regenerated from marrow mesenchymal stem cells express α_{1A} , α_{1B} , α_{1D} , β_1 , and β_2 adrenergic receptors and M_1 and M_2 muscarinic receptors [7]. Stimulation of the α_1 receptors with phenylephrine caused cardiomyocyte hypertrophy, and stimulation of the β receptors with isoproterenol increased the beating rate and contractility of the regenerated cardiomyocytes. These findings demonstrate the suitability of bone-marrow-derived regenerated cardiomyocytes as a candidate for use in cell transplantation therapy.

Purification of regenerated cardiomyocytes is required prior to use for cardiomyocyte transplantation. The population of cardiomyocytes in ES-cell-derived embryoid bodies is less than 10%, and the population of cardiomyocytes in 5-azacytidine-exposed CMG cells is less than 10–30%. To increase the efficiency of transplantation and protect recipients from possible adverse effects, regenerated cardiomyocytes need to be purified from the population of differentiated cell types prior to cell transplantation. Klug [8] and Muller [9] independently reported that embryonic stem-cell-derived cardiomyocytes could be purified using a cardiomyocyte-specific gene promoter–drug-resistant gene expression system. In this study, we purified bone-marrow-derived cardiomyocytes using a recombinant plasmid containing enhanced green fluorescent protein (EGFP) cDNA under the control of the myosin light chain-2v (MLC-2v) promoter. Purified cells were then transplanted into recipient mice hearts and the success of transplantation was analyzed histologically.

2. Methods

All experimental procedures and protocols were approved by the Animal Care and Use Committees of the Keio University, Japan, and the investigation conforms to the Guide for the Care and Use of Laboratory Animals published by the US National Institutes of Health (NIH Publication No. 85–23 revised 1996).

2.1. Preparation of bone marrow-derived regenerated cardiomyocytes

Murine bone-marrow-derived mesenchymal stem cells (CMG cells) were cultured in Iscove's modified

Dulbecco's medium (IMDM) supplemented with 20% FBS as previously described [6,7]. The cells were exposed to 3 $\mu\text{mol/l}$ of 5-azacytidine for 24 h to induce cell differentiation [6].

2.2. Construction of myosin light chain 2v-promoted EGFP plasmid

An expression vector, pMLC2v-EGFP, was constructed by cloning a 2.7-kb *HindIII*–*EcoRI* fragment of the rat MLC-2v promoter region [10,11] into the *HindIII*–*EcoRI* site of pEGFP-1 (Clontech, Palo Alto, CA), so that EGFP would be expressed under the control of MLC-2v promoter (Fig. 1a). This plasmid also contains the neomycin-resistance gene to enable selection of permanently transfected clones. MLC-2v is specifically expressed in ventricular cardiomyocytes.

2.3. Transfection of MLC2v-EGFP expression plasmid and cell selection

The MLC2v-EGFP plasmid was transfected into CMG cells by liposomal transfection. After 24 h when cells are about 20% confluent, a mixture containing 2 μg of plasmid DNA and 4 μl of LT1 TransIT Polyamine Transfection Reagent (Mirus Corporation) in OPTI-MEM (Life Technologies, Gaithersburg, MD) were added to each 35-mm culture dish. After selection with 1000 $\mu\text{g/ml}$ of G418 for 4 weeks, stably transfected colonies derived from single cells were cloned and pooled. EGFP fluorescence was observed under a fluorescence microscope (Olympus TMD300, Tokyo, Japan).

2.4. Flow cytometry and cell sorting

Flow cytometry and sorting of EGFP(+) cells were performed on a FACS Vantage (Becton Dickinson, Cockeysville, MD). Cells were analyzed by light forward and side scatter and for EGFP fluorescence through a 530 nm band pass filter as they traversed the beam of an argon ion laser (488 nm, 100 mW). Nontransfected control cells were used to set the background fluorescence. Cell sorting was performed 3 days after 5-azacytidine exposure at 500 cells/s as EGFP(+) cells displaying fluorescence higher than the background level were observed at this time point.

2.5. Infection of recombinant adenovirus vectors

Replication-deficient recombinant adenovirus vector, pAdex-LacZ, was constructed by cloning LacZ cDNA into the *SwaI* site of pAdex1CAwt as previously described [12]. In this vector, *E. coli* β -galactosidase is expressed under the control of a strong, ubiquitously expressed, promoter-derived from the cytomegalovirus enhancer-chicken β -actin hybrid [13]. On day 3 after seeding, EGFP(+) cells isolated by FACS were incubated

skeletal actin, α -cardiac actin, myosin light chain-2v (MLC-2v), MLC-2a, Cav1.2, myoD, calponin, and α -smooth muscle actin genes. The primers and PCR cycles used were as described previously [6,15,16]. Primers for Cav1.2 were CTGCAGGTGATGATGAGGTC for the forward primer and GCGGTGTTGTTGGCGTTGTT for the reverse primer.

2.9. Immunostaining

Cells were attached to gelatin-coated glass slides, fixed in 4% paraformaldehyde, and then stained with primary antibodies against anti-GATA4, anti-troponin I, and anti-MEF2C antibodies (all from Santa Cruz Biotechnology), or anti-connexin43 antibody (Sigma). Anti-goat-IgG conjugated with Texas red or anti-rabbit IgG conjugated with Rhodamine (1:500, Pharmingen) was used as a secondary antibody.

2.10. Action potential recording

Electrophysiological studies were performed in IMDM containing (mmol/L) CaCl₂ 1.49, KCl 4.23, and HEPES 25 (pH 7.4). Cultured cells were placed on the stage of an inverted phase contrast optic (Diaphoto-300, Nikon) at 23 °C. Action potentials were recorded using conventional microelectrodes as described previously [8]. Intracellular recordings were taken from MLC2v-EGFP-purified cells 3 weeks following transfection.

2.11. Cell transplantation

Animal Care and Use Committees of Keio University approved all experimental procedures and protocols. Female scid mice (12 weeks) were anesthetized initially with ether and placed on a warm pad maintained at 37 °C. The trachea was cannulated with a polyethylene tube connected to a respirator (Shinano, Tokyo, Japan) with a tidal volume set at 0.6 ml and a rate set at 110/min. Mice were then anesthetized with 0.5–1.5% isoflurane under controlled ventilation with a respirator for the remainder of the surgical procedure. A left thoracotomy was performed between ribs 4 and 5, and the pericardial sac was removed. Isolated EGFP(+) cells that had been expanded for 5 days were resuspended in PBS at a concentration of 5×10^7 cells/ml. A total cell suspension volume of 50 μ l was drawn into a 50 μ l Hamilton syringe with a 31-gauge needle, and 10 μ l was injected into the anterior wall of the left ventricle. Following the transplantation, residual cells in the syringe were collected and stained with trypan blue. The total and living cell numbers were counted. The number of living cells to inject was calculated by the following formula. (The injected living cells)=[(Total injected cells)–(Residual cells in the syringe)](Percent of living cells). Injection of PBS was used as a control.

2.12. Histological studies

The mice were sacrificed, and the hearts were dissected and fixed in 2% formaldehyde and 0.2% glutaraldehyde in PBS at room temperature for 5 min. The hearts were then washed in PBS and then incubated overnight in X-gal solution (1 mg/ml X-gal, 15 mmol/L potassium ferricyanide, 15 mmol/L potassium ferrocyanide, and 2 mmol/L MgCl₂ in PBS). The hearts were refixed in the same fix solution, embedded in paraffin, and sectioned into 6- μ m-thick slices for hematoxylin–eosin staining. The numbers of X-gal-stained CMG cells were counted using serial sections of the transplanted heart (more than 200 slices/mouse), and an estimate of total transplanted cell survival was obtained using the following formula. (Percent of cells surviving in the recipient heart)=[(Total surviving cells in the recipient heart)/(Injected living cells)]100.

To observe EGFP fluorescence, the hearts were embedded in OCT compound and frozen with liquid nitrogen. A cryostat was used to generate 6- μ m-thick sections. The samples were examined with a confocal LASER microscope (LSM510; Carl Zeiss, Jena, Germany). The GFP signal was confirmed by emission finger printing, using the LSM 510 Meta spectrometer (Carl Zeiss).

2.13. Electrocardiography (ECG) recording

ECG recordings were performed 2 and 4 weeks after transplantation. Mice were anesthetized with ether, needle limb leads were fixed, and the ECG was recorded for 1 h.

2.14. Statistics

Values are presented as mean \pm SD. The significance of differences among mean values was determined by ANOVA. Statistical comparison of the control and treated groups was carried out using the nonparametric Fisher's multiple comparison tests. The level accepted for significance was $p < 0.05$.

3. Results

3.1. Regenerated cardiomyocytes, but not other cell types, express EGFP

G418-resistant cells were exposed to 5-azacytidine and after 3 days EGFP(+) cells exhibited a fibroblast-like morphology (Fig. 1b,c), and were difficult to distinguish from other cell types. After 7 days, the EGFP(+) cells displayed a spindle-like morphology (Fig. 1d,e), but did not spontaneously beat at this stage. After 3 weeks, the EGFP(+) cells began to appear more rod-like and form inter-cell connections and after 4 weeks spontaneous beating was observed (Fig. 1f,g). Some fractions of the EGFP(–)

3.3. Character of the sorted EGFP(+) regenerated cardiomyocytes

A total of 768 single EGFP(+) cell clones were isolated using FACS analysis. Although EGFP(+) cells undergo cell division after 5-azacytidine exposure, a cardiomyocyte cell line could not be generated as cells stop proliferating after several cell divisions. The cells were exposed to BrdU to confirm their mitogenicity, and double immunostaining was performed with antisarcomeric myosin and anti-BrdU antibodies. Myosin-positive cells incorporated BrdU until day 5, but stopped incorporating it after day 7 (Fig. 3a). This finding shows that the mitogenicity of the isolated EGFP(+) CMG cells is limited, so it can be assumed that the risk of cardiomyosarcoma formation is negligible.

RT-PCR analysis of cardiac contractile proteins revealed that the isolated EGFP(+) CMG predominantly express the β -myosin heavy chain, α -skeletal-actin, and MLC-2v, indicating that the phenotype of these cells represents fetal ventricular cardiomyocytes. These cells also express cardiac L-type Ca^{2+} channels but did not express myogenic genes such as myoD, or smooth-muscle-specific genes, such as calponin or α -smooth muscle actin genes (Fig. 3b).

3.4. Action potential recording

MLC2v-EGFP-selected cells showed regular spontaneous beating 3 weeks following selection. The action potentials of these cells had a relatively shallow resting membrane potential with a late diastolic slow depolarization, like a pacemaker potential. They also displayed peak-notch-plateau characteristics representative of ventricular cardiomyocyte-like action potentials (Fig. 3c).

3.5. Immunostaining and transmission electron microscopy

Immunostaining revealed that EGFP(+) but not EGFP(-) CMG cells express cardiac troponin I (Fig. 4a–d). EGFP(+) CMG cells express both GATA4 and MEF2C, respectively (Fig. 4e,f). Interestingly, EGFP(-) CMG cells express GATA4 and Nkx2.5. These findings are consistent with the previous report that these cardiac transcription factors are expressed before final 5-azacytidine exposure [6]. EGFP(+) CMG cells also express connexin43 (Fig. 4g).

The sorted GFP(+) cells were cultured for 2 weeks, fixed, and processed for transmission electron microscopy. The typical contractile apparatus of the sarcomeres, including striation pattern, was observed (Fig. 4h).

3.6. Cell transplantation study

Animals with transplanted EGFP(+) cells were sacrificed at 2, 4, 8, and 12 weeks. Confocal LASER microscopy revealed that the EGFP(+) transplanted cardiomyocytes survived in the recipient heart (Fig. 5a–c). The control experiment revealed no EGFP(+) transplanted cardiomyo-

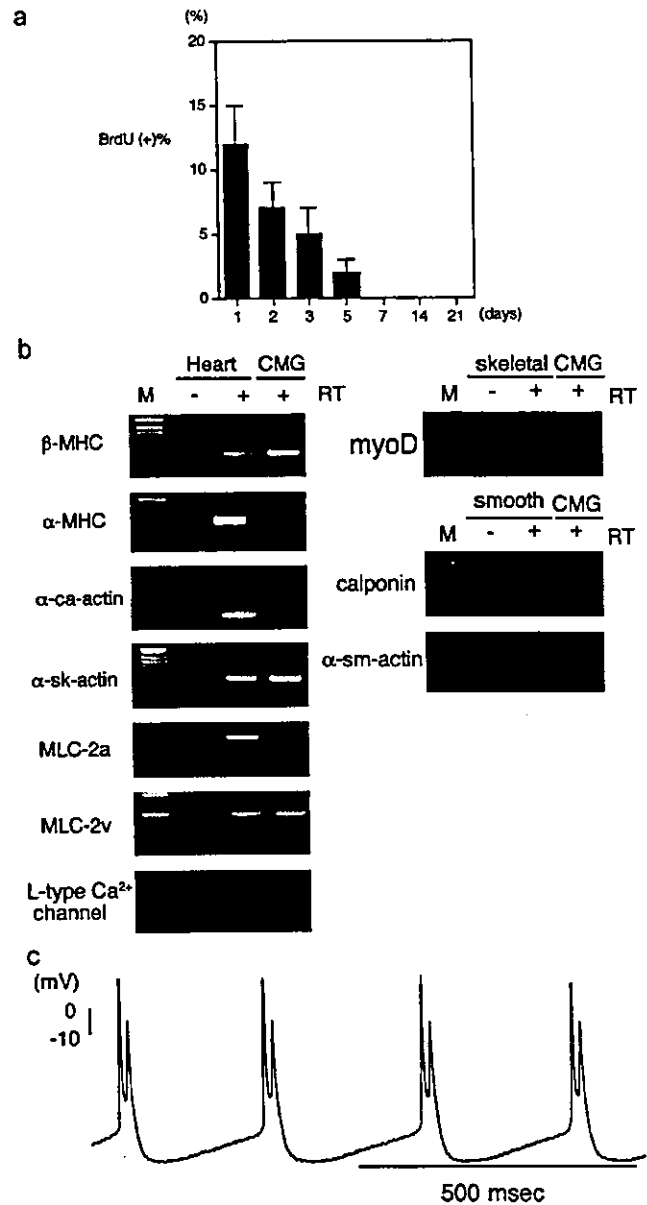


Fig. 3. Characteristics of the sorted CMG cardiomyocytes. (a) BrdU incorporation of EGFP(+) CMG cells after cell sorting. BrdU was loaded for 5 h, and its incorporation was detected. BrdU incorporation was observed until 5 days after cell sorting (8 days after 5-azacytidine exposure). (b) Phenotype of the EGFP(+) CMG cells. RT-PCR was performed for α -MHC, β -MHC, MLC-2v, MLC-2a, α -skeletal actin, α -cardiac actin, and cardiac α 1c Ca^{2+} channel. The expression pattern of the cardiac contractile protein indicated that these cells had the fetal ventricular phenotype. MLC-2v-EGFP selected cells did not express myoD, calponin, and α -smooth muscle actin genes. Femoral muscle, which includes vascular smooth muscle cells, were used as a positive control. M: 1-kb DNA ladder. RT: reverse transcription. (c) The representative tracing of the action potentials at 3 weeks after cell sorting was shown. These action potentials show ventricular cardiomyocyte-like action potentials.

cytes (data not shown) [17]. The orientation of the transplanted cells was consistent with the cardiomyocytes of the recipient heart. The EGFP(+) cells were observed only at the site of injection in the left ventricle and in no other parts of the heart. We also confirmed that these green signals were

A plasmid encoding reporter genes and cardiac specific gene promoters was used in a previous study to isolate cardiomyocytes from ES cells or embryonic carcinoma cells (EC cell) [21]. Klug et al. [8] transfected a fusion gene containing the α -myosin heavy chain (α -MHC) promoter and aminoglycoside phosphotransferase (NeoR) into pluripotent ES cells, then differentiated these cells in vitro prior to G418 selection. They reported high purification (>99%) and a survival period in the recipient heart of at least 7 weeks following transplantation. Zweigerdt et al. [22] and Zandstra et al. [23] reported a lab-scale protocol to generate cultures of highly enriched cardiomyocyte from ES cells transfected with a α -MHC-NeoR containing plasmid, and suggest its application to a larger-scale process for the supply of stem cell based cardiomyocytes. Muller et al. [9] isolated a subpopulation of ventricular-like cardiomyocytes from ES cells by transfecting the EGFP gene under the control of the MLC-2v promoter and cytomegalovirus enhancer. Moore et al. [24] reported that EC cell (P19C16)-derived cardiomyocytes could be isolated using an EGFP reporter under the control of 250 bp of the MLC-2v promoter. They enzymatically digested embryoid bodies, then isolated a population of cardiomyocytes (97% pure) using Percoll gradient centrifugation and FACS analysis. Kolossov et al. [25] reported the use of EGFP under the control of the cardiac α -actin promoter to isolate ES cell-derived cardiomyocytes. The present study confirmed the efficiency of this strategy for the isolation and purification of cardiomyocytes from bone-marrow-derived stem cells.

Reinecke and Murry [26] and Zhang et al. [27] highlighted the importance of a quantitative analysis of grafted cardiomyocytes, since a large number of fetal or neonatal cardiomyocytes often display apoptosis within several days of transplantation. They reported that only a small percentage of cardiomyocytes survive in the cryoinjured recipient heart, and that heat shock or adenoviral transfer of constitutive active Akt genes could increase their survival. In comparison, the present study reports a slightly higher survival rate for bone marrow-derived cardiomyocytes. One possible reason is the difference in the experimental models as the present study used a mouse uninjured model and not a rat cryoinjured heart model. Another reason is the small size of our not fully differentiated transplanted cells compared with fetal or neonatal cardiomyocytes. A small size may allow transplanted cells to go deep into the recipient heart without mechanical injury.

Recently, Takeda et al. [28] reported that the life span of human bone marrow mesenchymal stem cells could be prolonged by infecting the cells with the retrovirus encoding oncogene bmi-1, human papilloma virus E6 and E7, and human telomerase reverse transcriptase over 150 population doublings, and that these cells could be induced to differentiate into cardiomyocyte using 5-azacytidine and co-culture with the rat cardiomyocytes. Although this procedure is not suitable for clinical application at the present stage, the findings provide valuable information on the use

of human bone marrow stem cells for the regeneration of cardiomyocytes.

In summary, the present study provides a new model for tissue engineering. Further studies are required to improve cardiomyocyte differentiation and to increase the efficiency of the transplantation procedure.

Acknowledgements

This study was supported in part by the research grants (10B-1) of "Nervous and Mental Disorders from the Ministry of Health and Welfare", Japan, the research grants from the Ministry of Education, Science and Culture, Japan, and the research grants from Health Science Research Grants for Advanced Medical Technology from the Ministry of Welfare, Japan.

References

- [1] Leor J, Patterson M, Quinones MJ, Kedes LH, Kloner RA. Transplantation of fetal myocardial tissue into the infarcted myocardium of rat A potential method for repair of infarcted myocardium? *Circulation* 1996;94(Suppl. 9):II332–6.
- [2] Matsushita T, Oyamada M, Kurata H, Masuda S, Takahashi A, Emmoto T, et al. Formation of cell junctions between grafted and host cardiomyocytes at the border zone of rat myocardial infarction. *Circulation* 1999;100(Suppl. 19):II262–8.
- [3] Sakai T, Li RK, Weisel RD, Mickle DA, Kim EJ, Tomita S, et al. Autologous heart cell transplantation improves cardiac function after myocardial injury. *Ann Thorac Surg* 1999;68:2074–80.
- [4] Weissman IL. Translating stem and progenitor cell biology to the clinic: barriers and opportunities. *Science* 2000;287:1442–6.
- [5] Weissman IL, Anderson DJ, Gage F. Stem and progenitor cells: origins, phenotypes, lineage commitments, and transdifferentiations. *Annu Rev Cell Dev Biol* 2001;17:387–403.
- [6] Makino S, Fukuda K, Miyoshi S, Konishi F, Kodama H, Pan J, et al. Cardiomyocytes can be generated from marrow stromal cells in vitro. *J Clin Invest* 1999;103:697–705.
- [7] Hakuno D, Fukuda K, Makino S, Konishi F, Tomita Y, Manabe T, et al. Bone marrow-derived cardiomyocytes (CMG cell) expressed functionally active adrenergic and muscarinic receptors. *Circulation* 2002;105:380–6.
- [8] Klug MG, Soonpaa MH, Koh GY, Field LJ. Genetically selected cardiomyocytes from differentiating embryonic stem cells form stable intracardiac grafts. *J Clin Invest* 1996;98:216–24.
- [9] Muller M, Fleischmann BK, Selbert S, Ji GJ, Endl E, Middeler G, et al. Selection of ventricular-like cardiomyocytes from ES cells in vitro. *FASEB J* 2000;14:2540–8.
- [10] O'Brien TX, Lee KJ, Chien KR. Positional specification of ventricular myosin light chain 2 expression in the primitive murine heart tube. *Proc Natl Acad Sci U S A* 1993;90:5157–61.
- [11] Henderson SA, Spencer M, Sen A, Kumar C, Siddiqui MA, Chien KR. Structure, organization, and expression of the rat cardiac myosin light chain-2 gene. Identification of a 250-base pair fragment which confers cardiac-specific expression. *J Biol Chem* 1989;264:18142–8.
- [12] Kanegae Y, Makimura M, Saito I. A simple and efficient method for purification of infectious recombinant adenovirus. *Jpn J Med Sci Biol* 1995;47:157–66.
- [13] Niwa H, Yamamura K, Miyazaki J. Efficient selection for high-expression transfectants by a novel eukaryotic vector. *Gene* 1991;108:193–200.

Regenerative Medicine for Cardiomyocytes

JMAJ 47(7): 328–332, 2004

Keiichi FUKUDA

*Assistant Professor, Institute for Advanced Cardiac Therapeutics,
Keio University School of Medicine*

Abstract: Heart transplantation is the ultimate treatment option for severe cardiac failure, but is available only for a very small fraction of cases due to a serious donor shortage. Increasing attention has become focused upon a novel therapeutic approach, regenerative medicine, to break the present impasse. Attempts to regenerate cardiomyocytes have been made by using pluripotent embryonic stem cells or marrow-derived mesenchymal stem cells (adult stem cells). Cardiomyocytes can be regenerated from embryonic stem cells as well as from adult stem cells, but the regenerated cells differ in characteristics depending on the source stem cells. These two groups of stem cells differ with respect to proliferative potency, pluripotency, method of induction of differentiation into cardiomyocytes, rejection reactions, and tumorigenic potential. Further studies to ascertain which type of stem cell will be more useful and safer for this purpose remain to be carried out. Studies in laboratory animals have reportedly demonstrated improvement of cardiac function through regenerated cardiomyocyte transplantation into the heart, encouraging the hope that a new treatment modality has been found for severe heart failure.

Key words: Embryonic stem cell; Adult stem cell; Cardiomyocyte; Regenerative medicine

Introduction

In Japan, cases of heart disease have consistently been increasing with the aging of the population and the Westernization of the diet. A wide variety of pharmacotherapies has been developed for the treatment of intractable severe heart disease, with proven efficacy, however, heart transplantation is the sole radical

treatment option. There is still no increase in brain-dead donors and heart transplantation is a treatment available only for a very few cases.

To break the present impasse, therefore, a method to treat intractable cardiac failure by regenerating and transplanting cardiomyocytes is being sought. Studies of heart muscle cell regeneration have been making a steady progress, though at the level of laboratory ani-

This article is a revised English version of a paper originally published in the *Journal of the Japan Medical Association* (Vol. 129, No. 3, 2003, pages 365–368).

Table 1 Comparison of ES Cells and Adult Stem Cells as Materials for Regenerative Cardiomyocytes

	ES Cells	Adult Stem Cells
Origin	Post-fertilization early-stage embryo (inner cell mass of blastocyst)	Marrow stromal cell
Cell isolation technique, etc.	Method of cell establishment is already established, and is relatively easily performed.	Sparse among bone marrow cells, and method of cell establishment is yet to be established.
Proliferative potency	At present, cells are considered to infinitely proliferate.	Proliferate to some extent but the number of divisions is unknown.
Pluripotency	Differentiate into any type of cell <i>in vivo</i> . The cells differentiate into early developmental stage cells <i>in vitro</i> , but it is thought to be difficult for them to differentiate into cells that appear late in the fetal stage.	Recognized to be able to differentiate into mesodermal cells such as osteoblasts, chondroblasts and adipocytes, but reportedly undergo differentiation into nerve cells (ectoblast-derived) and cells of the liver (entoblast-derived) as well.
Differentiation into cardiomyocytes	Differentiate relatively easily, but a method to have ES cells specifically differentiate into cardiomyocytes has not been established.	Demonstrated to differentiate into cardiomyocytes, but a method to have the cells specifically differentiate into cardiomyocytes has not been established.
Rejection reactions	Occur	No rejection reactions if the cells are autologous.
Tumorigenic potential	There is potential risk of teratomas after transplantation if undifferentiated cells remain.	No

mal experiments, and will lead to development of research with human cells and their clinical application.

Stem cells currently used for regenerative medical therapy for the myocardium are broadly divided into two groups: embryonic stem cells (ES cells) obtained from early stage embryos post *in vitro* fertilization and marrow adult stem cells obtained from the bone marrow of adults. Whether one type is superior to the other for cardiomyocyte regeneration remains to be seen. Characteristics of the two types of stem cells are summarized in Table 1. This article outlines the current status and future prospects of regenerative medicine for the myocardium.

Differentiation from ES Cells to Cardiomyocytes

Figure 1 illustrates the outline of cardiomyocyte regeneration using ES cells. ES cells are those cells constituting the inner cell mass, destined to form the fetus, from an early

embryo having reached the stage of blastocyst. These cells are known to differentiate into any type of cell *in vivo* and have been shown to differentiate *in vitro* into a variety of organic cells such as cardiomyocytes, skeletal muscle cells, vascular endothelial cells, smooth muscle cells, neurons, and hepatocytes. However, most types of cells that appear late in the fetal stage have not been demonstrated from ES cells *in vitro*.

It is generally recognized that various cell growth factors, cytokines, and cell adhesion factors are required for ES cell differentiation into those various cells. Recent studies have clarified a cascade operating for selective differentiation of ES cells into motor neurons, however, the cascade for ES cell differentiation into cardiomyocytes has not been fully elucidated to date.

A method to have ES cells form a cell mass (embryoid) has been introduced as a general means of inducing ES cell differentiation into cells capable of differentiation. The frequency with which differentiation from the embryoid

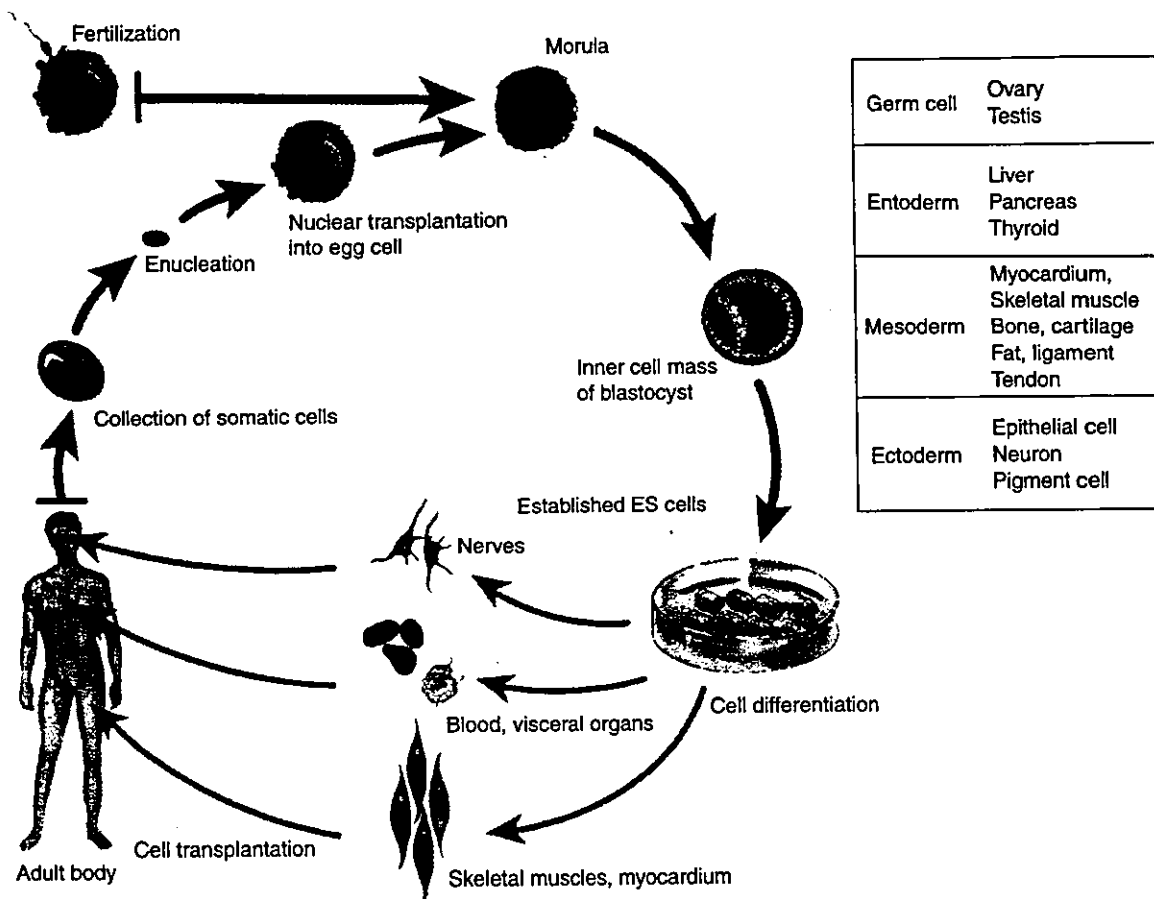


Fig. 1 Myocardial regeneration from ES cells

to cardiomyocytes is regarded as being about 7–8% at best. Humoral factors known to induce ES cell differentiation specifically into cardiomyocytes include bone morphogenetic protein-2 (BMP-2) and Wnt 11, which facilitate the differentiation, and Wnt 3 and Wnt 8, which act as inhibitors. Possible involvement of various other factors is presumed; the process seems to be quite intricate. Selective differentiation of ES cells into cardiomyocytes may become feasible from analysis of the pathways of the differentiation process.

Adult Stem Cell Differentiation into Cardiomyocytes

Bone marrow has been universally recognized to be the site of hematopoiesis with the

predominance of hematopoietic stem cells. In fact, more than 99% of marrow cells take part in the production and development of blood cells. It was discovered recently that, among bone marrow cells, there are cells termed stromal cells that essentially do not represent blood cells but secrete cytokines and growth factors to support cells of the hematopoietic system. The presence of pluripotent stem cells capable of differentiating into various types of cells among the marrow stromal cells has become recognized. These marrow stromal cells with pluripotent capacity are referred to as mesenchymal stem cells on account of their ability to differentiate into such mesenchymal cells as osteoblasts, chondroblasts, and adipocytes.

In view of the mesenchymal stem cells being

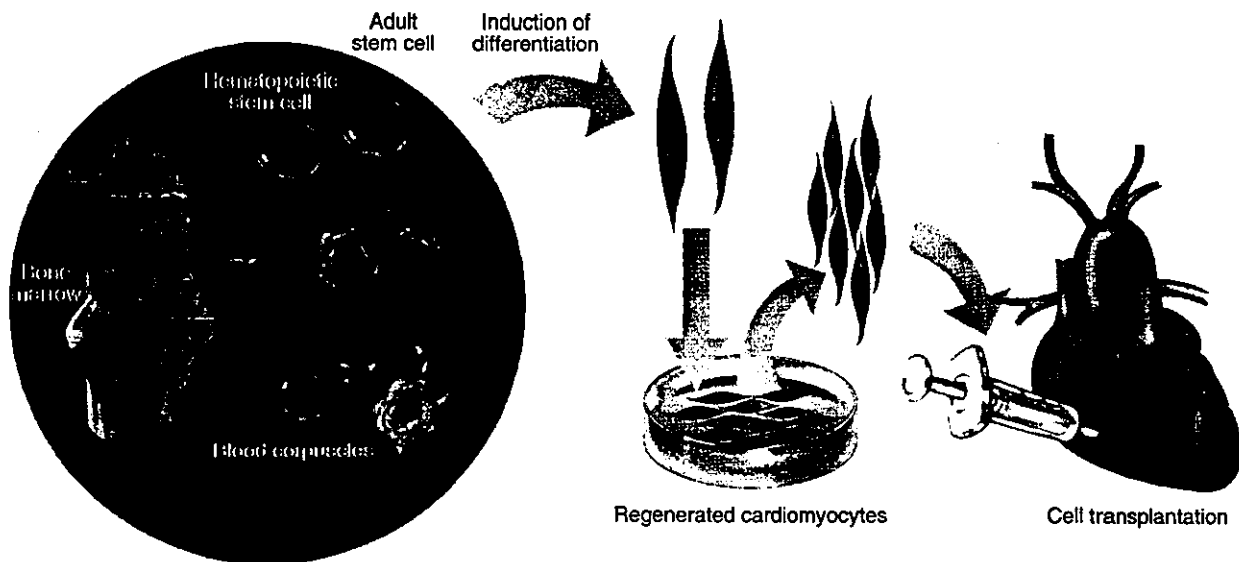


Fig. 2 Myocardial regeneration from adult stem cells and cell transplantation

able to differentiate into mesoblast-derived organs, we wondered if they could differentiate to become cardiomyocytes as well, which are also of mesodermal origin. Our studies demonstrated that cardiomyocytes that beat regularly by themselves can be obtained from mesenchymal stem cells. Figure 2 shows an outline of the process. Mesenchymal stem cells have recently been reported to undergo differentiation into nerve cells (ectoblast-derived) and cells of the liver (entoblast-derived) as well, and are now termed adult stem cells.

Characteristics of Regenerated Cardiomyocytes

Cardiomyocytes derived from bone marrow show expression of fetal ventricular muscle type genes soon after their differentiation from adult stem cells, and thereafter gradually express adult type genes.¹⁾ Expression of genes for atrial natriuretic polypeptide and cerebral natriuretic polypeptide that are considered cardiomyocyte-specific have also been demonstrated. The cells proved to self-beat, and those differentiated from murine adult stem cells showed 120–250 beats/min. The cardiomyo-

cytes exhibited the sinus node pattern of action potentials early after their differentiation from adult stem cells, and the pattern gradually changed to the ventricular muscle cell type.

Catecholamin α_1 receptor (cardiac hypertrophic effect) and β_1 and β_2 receptors (positive chronotropic and positive inotropic effects) play important roles in the muscle cells of the heart. In regenerated cardiomyocytes of bone marrow origin, α_1 receptor switched to myocardial type (mainly β_{1A} and β_{1B} receptors) as the differentiation proceeded into heart muscle cells, and simultaneously, β_1 and β_2 receptors that had not existed early in the course of differentiation became expressed.²⁾ Stimulation of these catecholamine receptors led to activation of subreceptor signaling to produce cardiac hypertrophy, increases in heart rate and increases in myocardial contractile force.

The above findings indicate that the regenerated cardiomyocytes are endowed with practically normal characteristics of cardiomyocytes.³⁾

Treatment of Cardiac Failure by Cell Transplantation

Cardiomyocyte transplantation has been